JOC Article
pubs.acs.org/joc

Fulleropyrrolidine End-Capped Molecular Wires for Molecular Electronics—Synthesis, Spectroscopic, Electrochemical, and Theoretical Characterization

Jakob Kryger Sørensen,[†] Jeppe Fock,[†] Anders Holmen Pedersen,[†] Asger B. Petersen,[†] Karsten Jennum,[†] Klaus Bechgaard,[†] Kristine Kilså,[†] Victor Geskin,*[,‡] Jérôme Cornil,[‡] Thomas Bjørnholm,[†] and Mogens Brøndsted Nielsen*[,†]

[†]*Department of Chemistry & Nano-Science Center, University of Copenhagen, Universitetsparken 5, DK-2100 Copenhagen Ø, Denmark, and* [‡]*Service de Chimie des Matériaux Nouveaux, University of Mons, Place du Parc 20, B-7000 Mons, Belgium*

victor.geskin@umons.ac.be; mbn@kiku.dk

Received October 20, 2010

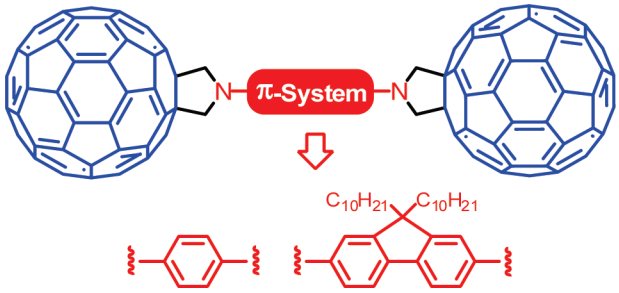

In continuation of previous studies showing promising metal−molecule contact properties a variety of C_{60} end-capped "molecular wires" for molecular electronics were prepared by variants of the Prato 1,3-dipolar cycloaddition reaction. Either benzene or fluorene was chosen as the central wire, and synthetic protocols for derivatives terminated with one or two fullero[*c*]pyrrolidine "electrode anchoring" groups were developed. An aryl-substituted aziridine could in some cases be employed directly as the azomethine ylide precursor for the Prato reaction without the need of having an electron-withdrawing ester group present. The effect of extending the π-system of the central wire from 1,4-phenylenediamine to 2,7-fluorenediamine was investigated by absorption, fluorescence, and electrochemical methods. The central wire and the C_{60} end-groups were found not to electronically communicate in the ground state. However, the fluorescence of C_{60} was quenched by charge transfer from the wire to C_{60}. Quantum chemical calculations predict and explain the collapse of coherent electronic transmission through one of the fulleropyrrolidine-terminated molecular wires.

Introduction

The development of so-called molecular wires for molecular electronics has attracted strong interest in recent years.[1] To employ a molecular wire in a device, it has to be placed between electrodes. One method is direct evaporation of the molecule into a nanogap.[2] However, manufacture of stable devices with wires fixed between electrodes requires "molecular alligator clips". Much work has focused on the preparation of molecular wires incorporating thiolate end-groups because these groups adhere strongly to gold.[3] However, thiols are known to have many different binding sites on gold, which leads to fluctuations in the electronic properties of the molecular junction.[4] We have turned our attention to using Buckminsterfullerene, C_{60}, as an anchoring group for

(1) (a) Reinerth, W. A.; Jones, L., II; Burgin, T. P.; Zhou, C.; Muller, C. J.; Deshpande, M. R.; Reed, M. A.; Tour, J. M. *Nanotechnology* **1988**, *9*, 246–250. (b) Tour, J. M. *Acc. Chem. Res.* **2000**, *33*, 791–804. (c) Pease, A. R.; Jeppesen, J. O.; Stoddart, J. F.; Luo, Y.; Collier, C. P.; Heath, J. R. *Acc. Chem. Res.* **2001**, *34*, 433–333. (d) Carroll, R. L.; Gorman, C. B. *Angew. Chem., Int. Ed.* **2002**, *41*, 4378–4400. (e) Robertson, N.; McGowan, C. A. *Chem. Soc. Rev.* **2003**, *32*, 96–103. (f) Rawlett, A. M.; Hopson, T. J.; Amlani, I.; Zhang, R.; Tresek, J.; Nagahara, L. A.; Tsui, R. K.; Goronkin, H. *Nanotechnology* **2003**, *14*, 377–384. (g) Marruccio, G.; Cingolani, R.; Rinaldi, R. *J. Mater. Chem.* **2004**, *14*, 542–554. (h) Flood, A. H.; Stoddart, J. F.; Steuerman, D. W.; Heath, J. R. *Science* **2004**, *306*, 2055–2056. (i) Nørgaard, K.; Bjørnholm, T. *Chem. Commun.* **2005**, 1812–1823. (j) Balzani, V.; Credi, A.; Venturi, M. *Chem.—Eur. J.* **2008**, *14*, 26–39. (k) Mayor, M. *Angew. Chem., Int. Ed.* **2009**, *48*, 5583–5585. (l) Moth-Poulsen, K.; Bjørnholm, T. *Nat. Nanotechnol.* **2009**, *4*, 551–556.

(2) Kubatkin, S.; Danilov, A.; Hjort, M.; Cornil, J.; Brédas, J.-L.; Stuhr-Hansen, N.; Hedegård, P.; Bjørnholm, T. *Nature* **2003**, *425*, 698–701.

(3) Nørgaard, K.; Nielsen, M. B.; Bjørnholm, T. In *Functional Organic Materials*; VCH-Wiley: Weinheim, Germany, 2007; pp 353−392.

DOI: 10.1021/jo102066x Published on Web 12/06/2010

CHART 1

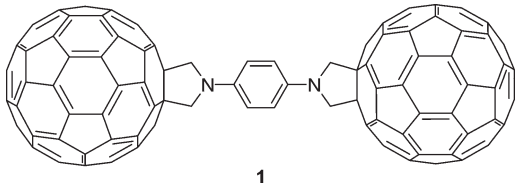

1

obtaining a more well-defined contact region to gold. C_{60} hybridizes strongly with gold surfaces[5] and allows for clear orientation-dependent mapping of frontier orbitals (HOMO, LUMO, LUMO+1) of C_{60} in STM experiments,[6] which implies resonant transmission through these orbitals at appropriate bias, and leads to single-molecule conductances on the order of one tenth of the conductance quantum.[7] Recently, some of us[8] have investigated the electrical characteristics of the C_{60} end-capped compound **1** (Chart 1) incorporated between two gold electrodes in a break junction. The studies revealed that in comparison to thiol anchoring, fullerene anchoring leads to a considerably lower spread in low-bias conductance. Furthermore, the experiments show that fullerene-anchored benzenes exhibited an increased stretching length before breaking. To further investigate the structure−property relations for this type of molecular wire we here present the detailed synthesis and characterization of the original dumbbell molecule/triad **1** as well as several new derivatives of these potential molecular wires comprising one or two C_{60} end-groups. We note that molecular wires incorporating a fullerene at one end and a thiol group at the other were recently reported by Tour and co-workers.[9] We have also performed quantum chemical calculations in order to assess the electron transport properties of such a triad in the coherent regime, in comparison to C_{60}. A molecular wire should ultimately ensure highly reproducible electronic communication between the metal electrodes to which it is connected. Since conductivity is not an intrinsic property of the molecule but of the entire junction including the molecule and the electrodes it is of paramount importance to control the metal molecule interface with atomic precision. In the case of the dumbbell molecules described here, this is achieved by the covalent bonds connecting the central wire to the C_{60} moieties.[8] To investigate how these specific bonds couple the wire to the electrodes we have studied theoretically how the coupling to metal through the C_{60} contact and whether electronic coupling between the constituent parts of the molecule is sufficient to allow for coherent electron transport. Even though we cannot yet include electron−electron correlations resulting in Coulomb blockade effects likely to play a role in this molecule the calculations shed light on the experimentally observed reduced molecular conductance of **1** in comparison to a single molecule of C_{60}.

In our synthetic approach, C_{60} is functionalized in a Prato reaction,[10] which is a 1,3-dipolar cycloaddition between C_{60} and an azomethine ylide generating a fulleropyrrolidine (Scheme 1). The ylide can be generated in situ either from a "condensation−decarboxylation route" in which a glycine derivative and paraformaldehyde are heated at reflux in toluene, or alternatively from thermal ring-opening of an aziridine derivative usually carrying an electron-withdrawing substituent. Here we will present convenient modifications of these methods.

Results and Discussion

Synthesis. The dumbbell **1** was synthesized by a 2-fold Prato reaction according to Scheme 2. First, *p*-phenylenediamine was treated with chloroacetic acid in water or DMF to furnish the diacid **3** according to previously reported procedures.[11] The azomethine ylide was generated in situ from **3** by condensation with formaldehyde followed by decarboxylation in refluxing toluene. Dumbbell **1** was isolated as a brown solid after repeated column chromatographic workup (to remove excess C_{60}). Not surprisingly, this compound suffered from limited solubility, but its identity was ascertained by both NMR spectroscopy and mass spectrometry. Purification of **3** was rather tedious, and a cleaner synthetic procedure was achieved by treating **2** with 2 molar equiv of diethyl dibromomalonate to yield **4** (Scheme 2) that was readily recrystallized from ethanol.[12] Hydrolysis under alkaline conditions followed by two decarboxylations gave compound **3**.

The complications regarding purification of the diacid **3** stimulated us to develop a new variant of the Prato reaction in which suitable solubilizing groups are removed in situ under the harsh cycloaddition conditions. This new protocol was employed for the synthesis of dumbbell **1** as shown in Scheme 3. Boc-protection of phenylenediamine **2** gave compound **5**. Deprotonation of this compound was now readily accomplished, which allowed alkylation with *tert*-butyl bromoacetate to furnish compound **6**. The advantage of this protocol is that both compounds **5** and **6** were easy to purify, and the Boc groups enhance the stability by decreasing the reducing power of the molecule (i.e., it is less prone to oxidation). Refluxing **6** with paraformaldehyde and C_{60} in 1-chloronaphthalene gave **1** in a yield of 5%; thus, both the carbamates and ester groups are conveniently cleaved under the reaction conditions.

(4) (a) Moore, A. M.; Dameron, A. A.; Mantooth, B. A.; Smith, R. K.; Fuchs, D. J.; Ciszek, J. W.; Maya, F.; Yao, Y.; Tour, J. M.; Weiss, P. S. *J. Am. Chem. Soc.* **2006**, *128*, 1959–1967. (b) Ulrich, J.; Esrail, D.; Pontius, W.; Venkataraman, L.; Millar, D.; Doerrer, L. H. *J. Phys. Chem. B* **2006**, *110*, 2462–2466. (c) Li, C.; Pobelov, I.; Wandlowski, T.; Bagrets, A.; Arnold, A.; Evers, F. *J. Am. Chem. Soc.* **2008**, *130*, 318–326.

(5) Rogero, C.; Pascual, J. I.; Gómez-Herrero, J.; Baró, A. M. *J. Chem. Phys.* **2002**, *116*, 832–836.

(6) (a) Lu, X.; Grobis, M.; Khoo, K. H.; Louie, S. G.; Crommie, M. F. *Phys. Rev. Lett.* **2003**, *90*, 096802. (b) Lu, X.; Grobis, M.; Khoo, K. H.; Louie, S. G.; Crommie, M. F. *Phys. Rev. B.* **2004**, *70*, 115418. (c) De Menech, M.; Saalmann, U.; Garcia, M. E. *Phys. Rev. B* **2006**, *73*, 155407. (d) Torrente, I. F.; Franke, K. J.; Pascual, J. I. *J. Phys.: Condens. Matter* **2008**, *20*, 184001. (e) Schull, G.; Néel, N.; Becker, M.; Kröger, J.; Berndt, R. *New J. Phys.* **2008**, *10*, 065012. (f) Larsson, J. A.; Elliott, S. D.; Greer, J. C.; Repp, J.; Meyer, G.; Allenspach, R. *Phys. Rev. B* **2008**, *77*, 115434.

(7) Böhler, T.; Edtbauer, A.; Scheer, E. *Phys. Rev. B* **2007**, *76*, 125432.

(8) Martin, C. A.; Ding, D.; Sørensen, J. K.; Bjørnholm, T.; van Ruitenbeek, J. M.; van der Zant, H. S. J. *J. Am. Chem. Soc.* **2008**, *130*, 13198–13199.

(9) Shirai, Y.; Guerrero, J. M.; Sasaki, T.; He, T.; Ding, H.; Vives, G.; Yu, B.-C.; Cheng, L.; Flatt, A. K.; Taylor, P. G.; Gao, Y.; Tour, J. M. *J. Org. Chem.* **2009**, *74*, 7885–7897.

(10) (a) Maggini, M.; Scorrano, G.; Bianco, A.; Toniolo, C.; Sijbesma, R. P.; Wudl, F.; Prato, M. *J. Chem. Soc., Chem. Soc.* **1994**, 305–306. (b) Prato, M.; Maggini, M.; Giacometti, C.; Scorrano, G.; Sandonà, G.; Farnia, G. *Tetrahedron* **1996**, *52*, 5221–5234. (c) Prato, M.; Maggini, M. *Acc. Chem. Res.* **1998**, *31*, 519–526. (d) Tagmatarchis, N.; Prato, M. *Synlett* **2003**, 768–779.

(11) (a) Fränkel, S.; Bruckner, F. *Chem. Ber.* **1916**, *49*, 485–488. (b) Zimmermann, J.; Knyrim, M. *Chem Ber.* **1883**, *16*, 514–516.

(12) Ruggli, P.; Grand, R. *Helv. Chim. Acta* **1937**, *20*, 373–386.

SCHEME 1. Variants of the Prato Reaction

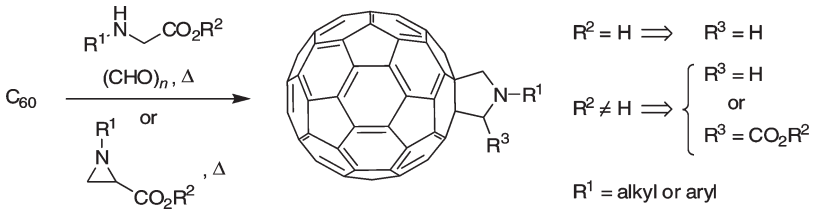

SCHEME 2. Synthetic Route to Molecular Dumbbell 1[a]

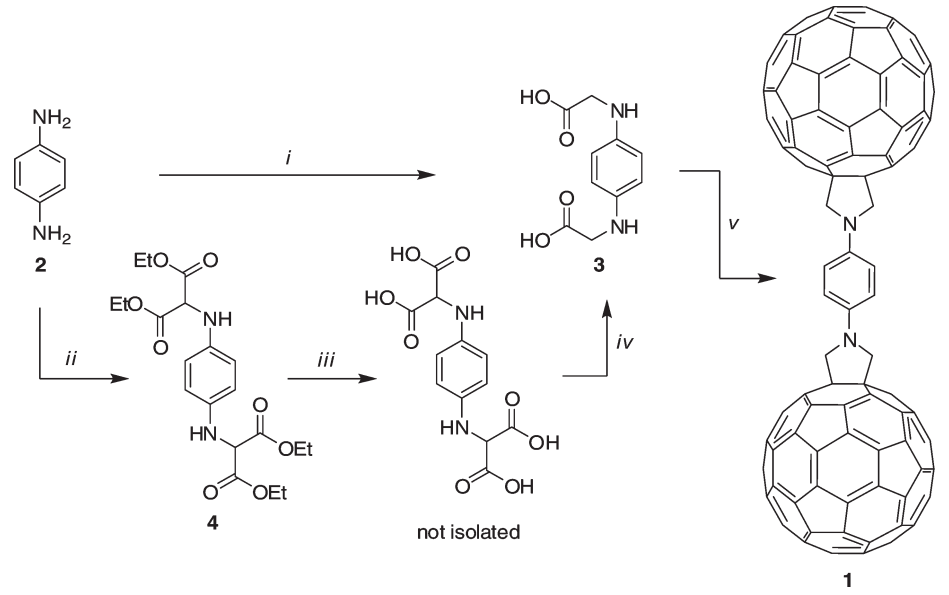

[a]Conditions: (i) $ClCH_2CO_2H$, DMF, K_2CO_3. (ii) DMF, diethyl bromomalonate, K_2CO_3. (iii) KOH, H_2O, reflux. (iv) HCl (aq). (v) C_{60}, $(CHO)_n$, 1,2-dichlorobenzene, reflux; 5%.

As a useful reference compound for spectroscopic and electrochemical studies (vide infra), we synthesized the known compound **7**[13] (Chart 2) incorporating only one C_{60} unit. Another derivative with only one C_{60} end-group was prepared according to Scheme 4. Here an aziridine was chosen as precursor for the azomethine ylide. First, 4-bromonitrobenzene (**8**) was treated with 1-octyne in a Sonogashira cross-coupling reaction[14] to furnish the product **9** in high yield. The nitro and alkyne groups were then reduced by molecular hydrogen and palladium on carbon to provide 4-octylaniline (**10**).[15] This aniline incorporating a solubilizing alkyl group was subsequently treated with 2-chloroacetylchloride to give the 2-chloroacetamide **11**. According to Potier et al.,[16] reduction of 2-chloroacetamides and ring closure to the corresponding *N*-substituted aziridine is possible in one step using alane in THF. We were, however, not able to generate the aziridine in this manner from **11**. Instead, compound **11** was reduced to the corresponding amine **12** by using borane−dimethyl sulfide complex in THF and the 2-chloroethylamine (**12**) was subsequently cyclized by using sodium hydride in DMSO.

SCHEME 3. Alternative Route to Molecular Dumbbell 1[a]

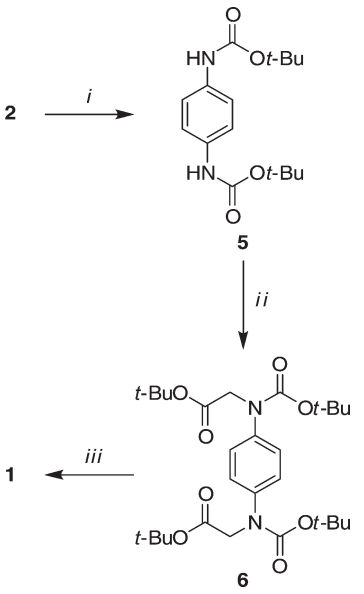

[a]Conditions: (i) Boc_2O, NEt_3, CH_2Cl_2; 51%. (ii) $BrCH_2CO_2t$-Bu, NaH, DMF; 76%. (iii) C_{60}, $(CHO)_n$, 1-chloronaphthalene, reflux; 5%.

(13) Maggini, M.; Scorrano, G.; Prato, M. *J. Am. Chem. Soc.* **1993**, *115*, 9798–9799.

(14) Sonogashira, K.; Tohda, Y.; Hagihara, N. *Tetrahedron Lett.* **1975**, 4467–4470.

(15) For alternative syntheses of 4-octylaniline, see: (a) Gedye, R. N.; Bozic, J.; Durbano, P. M.; Williamson, B. *Talanta* **1989**, *36*, 1055–1058. (b) Manolikakes, G.; Hernandez, C. M.; Schade, M. A.; Metzger, A.; Knochel, P. *J. Org. Chem.* **2008**, *73*, 8422–8436.

(16) (a) Langlois, Y.; Husson, H.; Potier, P. *Tetrahedron Lett.* **1969**, *10*, 2085–2088. (b) Langlois, Y.; Poupat, C.; Husson, H.; Potier, P. *Tetrahedron* **1970**, *26*, 1967–1976.

CHART 2

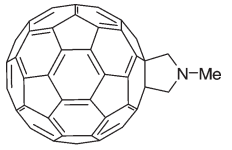

7

SCHEME 4. Synthesis of "Half-Dumbbell"[a]

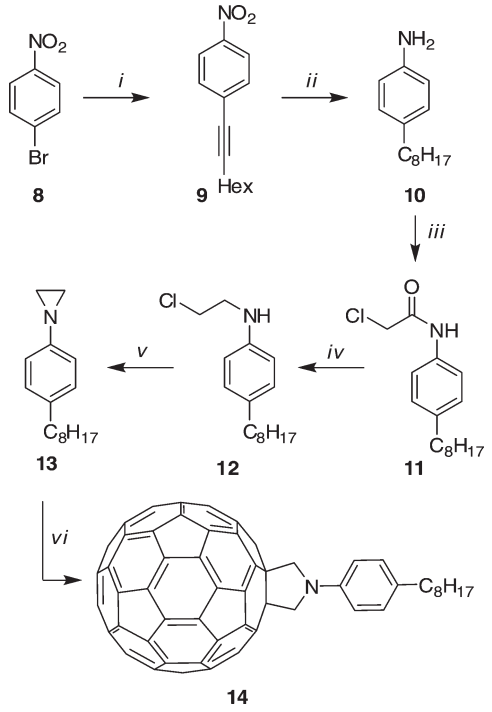

[a]Conditions: (i) 1-Octyne, $[Pd(PPh_3)_2Cl_2]$, CuI, MeCN, Et_3N; 99%. (ii) H_2 (g), Pd/C, EtOAc; 67%. (iii) Chloroacetyl chloride, K_2CO_3, DMF; 76%. (iv) BH_3-SMe_2, THF; 82%. (v) NaH, DMSO; 49%. (vi) C_{60}, 1,2-dichlorobenzene, 200 °C; 28%.

Thermal ring-opening of the aziridine **13** to an azomethine ylide followed by in situ cycloaddition with C_{60} was tested with several solvents (benzene, toluene, *o*-xylene, *m*-xylene, chlorobenzene, 1,2-dichlorobenzene, 1-chloronaphthalene, decalin, and diphenyl ether) and at several temperatures (100, 150, 200, 250, and 300 °C). 1,2-Dichlorobenzene at 250 °C was found to provide the optimum conditions for obtaining the desired fulleropyrrolidine **14**. A yield of 28% was obtained after repeated column chromatographic purification. To our knowledge, this is the first example of functionalizing C_{60} by treatment with an aziridine containing only an *N*-substituent, while several examples are known from the literature using azidirines with a substituent at C-2,[17] most often an electron-withdrawing ester substituent group.

(17) (a) Bianco, A.; Gasparrini, F.; Maggini, M.; Misiti, D.; Polese, A.; Prato, M.; Scorrano, G.; Toniolo, C.; Villani, C. *J. Am. Chem. Soc.* **1997**, *119*, 7550–7554. (b) Thomas, K. G.; Biju, V.; George, M. V.; Guldi, D. M.; Kamat, P. V. *J. Phys. Chem. A* **1998**, *102*, 5341–5348. (c) Gasparrini, F.; Misiti, D.; Negra, F. D.; Maggini, M.; Scorrano, G.; Villani, C. *Tetrahedron* **2001**, *57*, 6997–7002. (d) Bianco, A.; Maggini, M.; Nogarole, M.; Scorrano, G. *Eur. J. Org. Chem.* **2006**, 2934–2941.

SCHEME 5. Synthesis of 14 and 16[a]

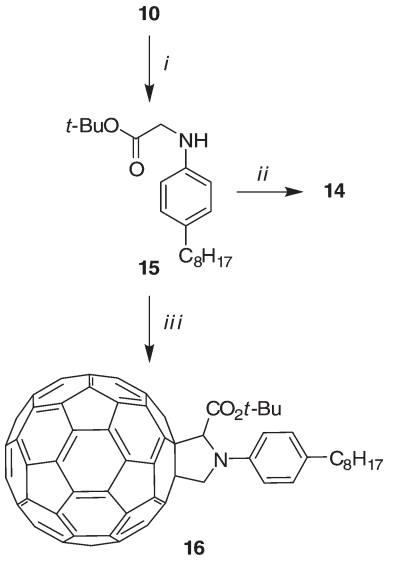

[a]Conditions: (i) $BrCH_2CO_2t$-Bu, DMF, K_2CO_3, rt, overnight; 70%. (ii) C_{60}, $(CH_2O)_n$, *p*-TsOH, 1-chloronaphthalene, reflux; 25%. (iii) C_{60}, $(CH_2O)_n$, 1,2-dichlorobenzene, 130 °C; 8%.

SCHEME 6. Synthesis of 18 and 19[a]

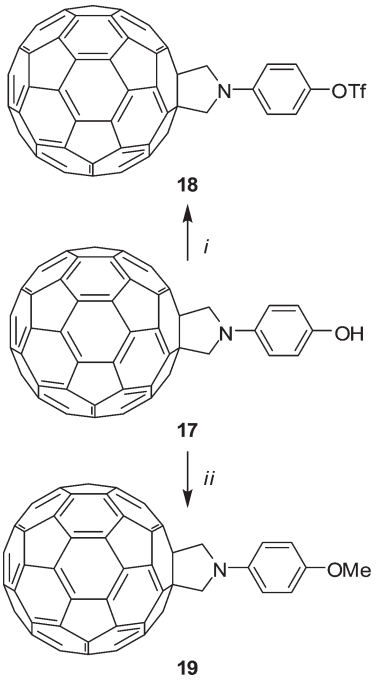

[a]Conditions: (i) Tf_2O, toluene, pyridine, rt; 90%. (ii) K_2CO_3, MeI, DMF/THF; 30%.

The Prato reaction was also performed from the *tert*-butyl ester **15**, readily prepared from the aniline derivative **10** (Scheme 5). Upon heating of **15** to 250 °C in 1-chloronaphthalene, the product **14** was formed. Decarboxylation was avoided by heating to 150 °C in 1,2-dichlorobenzene, providing the product **16**.

Next, a selection of phenol derivatives with one C_{60} anchoring group was prepared. The phenol **17** (Scheme 6)

SCHEME 7. Attempted Synthesis of Dumbbell[a]

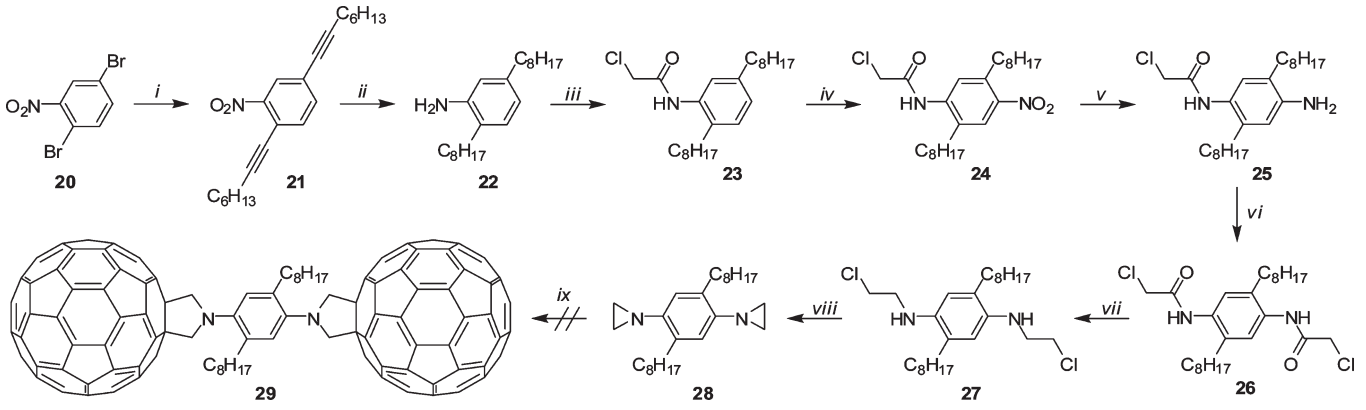

[a]Conditions: (i) 1-Octyne, $[Pd(PPh_3)_2Cl_2]$, CuI, THF, Et_3N, DMF; 80%. (ii) H_2 (g), Pd/C, EtOAc, MeOH; 95%. (iii) $ClCH_2COCl$, K_2CO_3, DMF, 0 °C → rt; 61%. (iv) H_2SO_4/HNO_3, CH_3CO_2H, 0→55 °C; 45%. (v) Diethylviologene dibromide, K_2CO_3, $Na_2S_2O_4$, CH_2Cl_2, H_2O, 50 °C; 39%. (vi) $(ClCH_2CO)_2O$, CH_2Cl_2, rt; 71%. (vii) $BH_3 \cdot Me_2S$, THF, 0 °C→rt; 83%. (viii) NaH, DMSO, 50 °C; ca. 100%. (ix) C_{60}, 1-chloronaphthalene, 250 °C; 0%.

was prepared according to a literature protocol.[18] It was converted into the triflate **18** upon treatment with triflic anhydride in a mixture of toluene and pyridine (Scheme 6). This triflate could potentially be employed as a building block for palladium-catalyzed cross-coupling reactions. The anisol derivative **19** was prepared by methylation of the phenolate generated from **17** (Scheme 6).

Our next objective was to functionalize the phenylenediamine unit of dumbbell **1** with alkyl groups in order to enhance the solubility. Unfortunately, this functionalization also increased the instability of the compound (presumably owing to the enhanced donor strength of phenylenediamine). The attempted synthesis is shown in Scheme 7 and is based on a phenylenediaziridine as the immediate precursor for the dumbbell. Despite the fact that the final dumbbell was not accomplished, the synthesis has provided several interesting aniline and phenylenediamine derivatives that may be useful for related work. The dibromide **20** was subjected to a 2-fold Sonogashira cross-coupling reaction with 1-octyne to provide the product **21**. The alkyne and nitro groups were then reduced in a hydrogenation reaction to furnish the aniline **22**. This compound was functionalized with a chloroacetyl group to afford **23** that was then nitrated to furnish **24**. The nitro group was reduced to give the phenylenediamine **25**. Next, a second chloroacetyl group was incorporated to furnish **26**. The two amide functionalities were reduced by borane−dimethyl sulfide complex to provide compound **27** that was converted into the bis-aziridine **28** upon treatment with sodium hydride. Finally, a 2-fold Prato reaction was attempted in order to obtain the dumbbell **29**, but even after several attempts we did not manage to isolate any product corresponding to **29**. To expand the potential scope of the aniline **22**, it was iodinated by using benzyltrimethylammonium dichloroiodate ($BTMA \cdot ICl_2$) (Scheme 8). The resulting product **30** served as precursor for the acetylenic compound **31** by subjecting it to a Sonogashira cross-coupling reaction with triisopropylsilylacetylene under microwave heating. The aniline **30** was also treated with *tert*-butyl bromoacetate to furnish compound **32**. Compounds **31** and

SCHEME 8. Synthesis of 31 and 32[a]

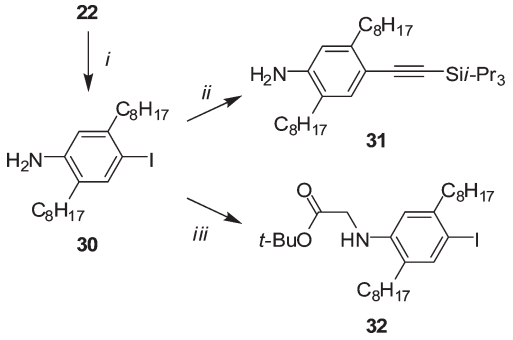

[a]Conditions: (i) $BTMA \cdot ICl_2$, $NaHCO_3$, CH_2Cl_2, MeOH, 0 °C; 80%. (ii) Triisopropylsilylacetylene, $[Pd(PPh_3)_2Cl_2]$, CuI, THF, $HNi\text{-}Pr_2$; 100 °C (μw); 90%. (iii) $t\text{-}BuO_2CCH_2Br$, K_2CO_3, DMF, 60 °C; 75%.

32 might be explored in future work as building blocks in the field of acetylenic scaffolding[19] or for Prato reactions.

The results described above have shown that the Prato cycloaddition reaction can be accomplished from a phenylaziridine but not from a phenylenediaziridine with alkyl groups attached. We reckoned that it might be possible to perform the 2-fold Prato reaction from a diaziridine if a more stable aromatic unit is employed. For this purpose we chose a central fluorene unit. This unit is also interesting for other reasons. While steric constraints limit coplanarity in biphenyls, coplanarity between the two aromatic rings is enforced in fluorene. As shown by Mayor, Wandlowski, and coworkers[20] the value of the torsion angle between the phenyl rings in biphenyls relates to the molecular conductance. The successful synthesis of a fluorene dumbbell using the aziridine protocol is shown in Scheme 9. Functionalization of the

(18) Kang, S. H.; Ma, H.; Kang, M.-S.; Kim, K.-S.; Jen, A. K.-Y.; Zareie, H.; Sarikaya, M. *Angew. Chem., Int. Ed.* **2004**, *43*, 1512–1516.

(19) For reviews on the scope of acetylenic scaffolding, see: (a) Tykwinski, R. R.; Diederich, F. *Liebigs Ann./Recl.* **1997**, 649–661. (b) Diederich, F. *Chem. Commun.* **2001**, 219–227. (c) Tykwinski, R. R.; Zhao, Y. M. *Synlett* **2002**, 1939–1953. (d) Nielsen, M. B.; Diederich, F. *Chem. Rec.* **2002**, *2*, 189–198. (e) Nielsen, M. B.; Diederich, F. *Synlett* **2002**, 544–552. (f) Fallis, A. G. *Synlett* **2004**, 2249–2267. (g) Nielsen, M. B.; Diederich, F. *Chem. Rev.* **2005**, *105*, 1837–1867.

(20) Mishchenko, A.; Vonlanthen, D.; Meded, V.; Bürkle, M.; Li, C.; Pobelov, I. V.; Bagrets, A.; Viljas, J. K.; Pauly, F.; Evers, F.; Mayor, M.; Wandlowski, T. *Nano Lett.* **2010**, *10*, 156–163.

SCHEME 9. Synthesis of 40[a]

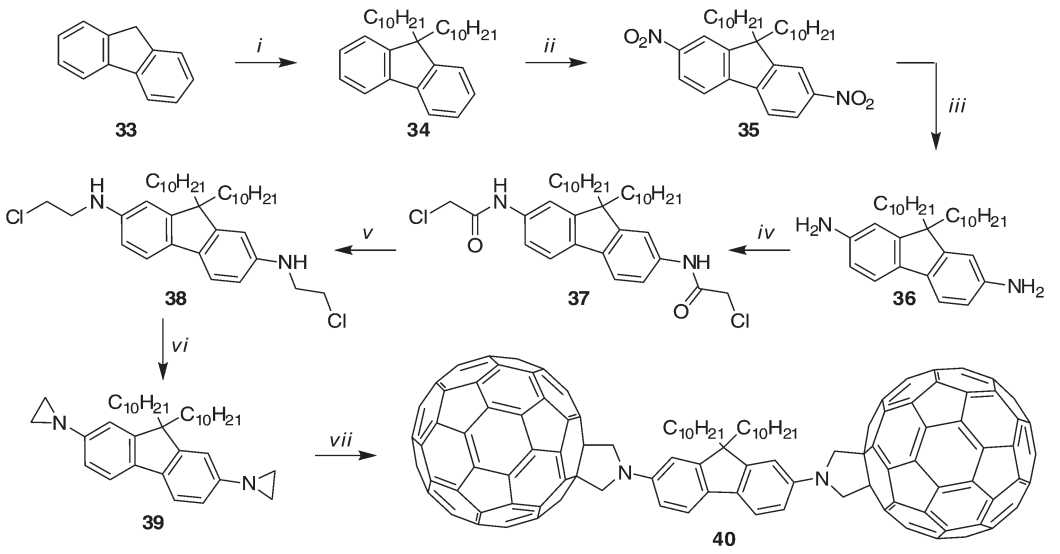

[a]Conditions: (i) DMF, NaH, decylbromide; 75%. (ii) HNO_3, H_2SO_4; 50%. (iii) EtOAc, Pd/C, H_2 (4 bar); 89%. (iv) DMF, K_2CO_3, chloroacetyl chloride; 96%. (v) BH_3-SMe_2, THF; 75%. (vi) DMF, NaH. (vii) 1,2-dichlorobenzene, C_{60}, reflux; 5%.

fluorene **33** with two decyl groups proceeded according to a similar procedure previously reported.[21] The dialkylated product **34** was regioselectively nitrated according to a related literature procedure[22] to yield the dinitro compound **35** that was reduced to the diamine **36** in excellent yield by using palladium on carbon and molecular hydrogen. The diamine appeared as a brown oil that turned black in a few days, and therefore acylation with chloroacetyl chloride had to be carried out as quickly as possible. Acylation with chloroacetyl chloride gave **37**, which was reduced to the chloroethylamine **38**. The ring closure to afford the bis-aziridine **39** was performed in a similar way as described above. The final cycloaddition reaction was carried out in 1,2-dichlorobenzene at reflux and gave, gratifyingly, the product **40**, albeit in an overall yield of only 5%. Yet, the yield corresponds to 22% for each of the two cycloaddition reactions. The solubility of the bis(fulleropyrrolidine)fluorene **40** was appreciably higher than that of **1**.

A similar protocol to that depicted in Scheme 3 ("carbamate route") could also be employed for preparing the fluorene dumbbell **40** according to Scheme 10. Thus, Boc-protection of **36** gave compound **41** in high yield. This compound was then alkylated with *tert*-butyl bromoacetate in the presence of sodium hydride as base to provide compound **42**. It should be noted that direct alkylation of the fluorenediamine **36** with *tert*-butyl bromoacetate gave an unstable product that could not be purified without decomposition. The presence of Boc groups in **42** renders this compound perfectly stable. Finally, treatment with C_{60} and paraformaldehyde in chloronaphthalene gave the dumbbell **40** in a yield of 14%, corresponding to a yield of 37% for each Prato reaction. Thus, this protocol is more efficient than the "aziridine protocol" described above.

SCHEME 10. Alternative Route to Fluorene Dumbbell 40[a]

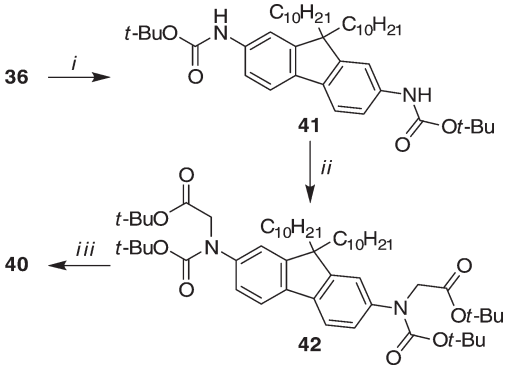

[a]Conditions: (i) Boc_2O, K_2CO_3, dioxane; 92%. (ii) $BrCH_2CO_2t$-Bu, NaH, DMF; 82%. (iii) C_{60}, $(CHO)_n$, 1-chloronaphthalene, reflux; 14%.

Physicochemical Properties. We will first consider the ground-state electrochemistry of the compounds. Thereafter the absorption and emission spectroscopy of the neutral species will be presented. These experiments will reveal the possibility of excited state electron transfer. Finally, spectroelectrochemistry will reveal the absorption characteristics of reduced and oxidized species, and the results will be compared to chemical oxidation of the central phenylenediamine wire of **1**. The aim of these studies is to judge the reasonableness of charge transfer. Compound **7** (*N*-methylfulleropyrrolidine) will be looked upon as a reference compound for systems **14** and **19** in which the pyrrolidine is extended to more electron-donating groups, and in particular as a reference for dumbbells **1** and **40** which are systems containing an electron donor moiety between two fullerenes.

Electrochemistry. The redox properties of the new C_{60} compounds were investigated by cyclic voltammetry (CV) and square-wave voltammetry (SWV) in a 1:2 mixture of acetonitrile and 1,2-dichlorobenzene (DCB). Owing to the limited solubility, the CV of **1** showed rather small signals.

(21) Tsuie, B.; Reddinger, J. L.; Sotzing, G. A.; Soloducho, J.; Katritzky, A. R.; Reynolds, J. R. *J. Mater. Chem.* **1999**, *9*, 2189–2200.

(22) Brisse, F.; Durocher, G.; Gauthier, S.; Gravel, D.; Marques, R.; Vergelati, C.; Zelent, B. *J. Am. Chem. Soc.* **1986**, *108*, 6579–6586.

TABLE 1. Cyclic Voltammetric Data (Half-Wave Potentials) and Square-Wave Voltammetry Data (in Parentheses)

compd	potentials vs Fc^+/Fc					
C_{60}	−0.97 (−0.97)	−1.37 (−1.37)	−1.84 (−1.84)	−2.29 (−2.30)		
p-$(Me_2N)_2C_6H_4$					−0.30 (−0.25)	+0.30[a] (+0.40)
1	−1.15 (−1.15)	−1.50 (−1.51)	−2.04 (−2.05)		+0.14 (+0.17)	+0.54[b] (+0.57)
7	−1.08 (−1.08)	−1.47 (−1.47)	−2.01 (−2.01)			
14	−1.05 (−0.93)	−1.45 (1.32)	−1.99 (−1.85)	−2.42	+0.62[c]	
17	−1.06 (−1.06)	−1.47 (−1.37)[d]	−1.99 (−1.99)[d]		+0.29 (+0.20)	(+0.36)
18	−1.10 (−1.08)	−1.50 (−1.48)	−2.04 (−2.02)		+0.2 (+0.21)[e]	
19	−1.05 (−1.05)	−1.44 (−1.44)	−1.97 (−1.98)		+0.42 (+0.43)	
39[f]					+0.47 (+0.48)	+0.69 (+0.71)
40	−1.06 (−1.09)	−1.46 (−1.5)[d]	−1.99 (−2.03)[d]		+0.22 (−0.01)[g]	+0.39 (+0.2)[g]
43[h]	−1.06 (−1.06)	−1.45 (−1.45)	−1.99 (−1.99)	(−2.34)	+0.32 (+0.33)	+0.45 (+0.43)

[a]Only reversible at high scan rates. [b]Anodic peak (irreversible). [c]Anodic peak approximately twice the size of the cathodic peak. [d]EC at second peak (possibly protonation of C_{60}); thus, all peaks at lower potentials are perturbed. [e]Quasireversible. [f]EC reaction, probably ring-opening of the three-membered ring. [g]Irreversible oxidations (quasireversible at high scan rates; the oxidation at +0.4 V is not seen in SWV). [h]The waves at positive potential are smaller than the waves at negative potential.

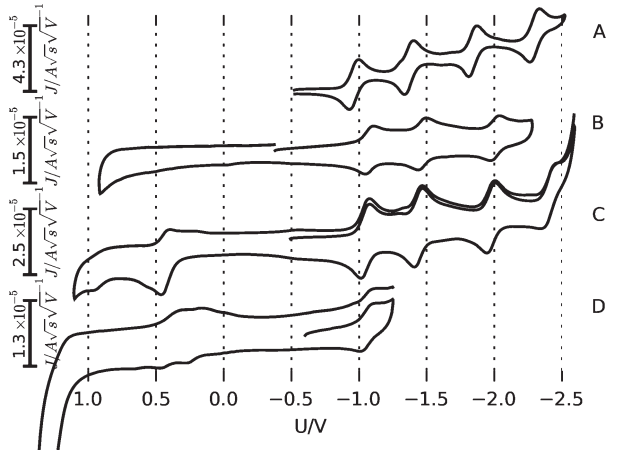

FIGURE 1. Cyclic voltammograms reported against Fc^+/Fc of (A) C_{60}, (B) **7**, (C) **19**, and (D) **40**. Only the first reduction wave of **40** is shown as the second included a chemical reaction (possible hydrogenation from an impurity in the solution).

The redox potentials are listed in Table 1 and some representative CVs are shown in Figure 1. Owing to the use of the MeCN/DCB solvent mixture having a more limited potential window than MeCN, only four reversible waves were observed for C_{60}, while six reversible waves are normally observed in MeCN/toluene.[23] Introduction of the pyrrolidine unit resulted in a slight decrease of the electron acceptor strength of C_{60}, which is explained by the small disruption of the conjugation. No oxidation wave was seen for **7**, while compounds **14**, **1**, **17**, **18**, and **19**, incorporating either aniline, phenylenediamine, or phenol electron donors, showed one or two oxidation steps. Notably, the fluorene derivative **39** was oxidized at rather high potentials compared to those of the fluorene dumbbell **40**. Thus, the aziridine ring diminishes the donor strength of the "fluorenediamine" significantly. In line with this observation, the fluorene **43** (Chart 3) containing one C_{60} and one aziridine end-group, isolated as a byproduct in the synthesis of **40**, was oxidized at potentials intermediate between those of **39** and **40**.

Calculation of Free Energy for Charge Transfer. The measured redox potentials together with estimates of electrostatic energies can be used to estimate the free energy and

CHART 3

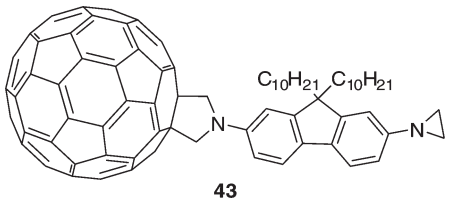

43

thus the possibility of charge transfer in the ground state. On account of the intramolecular nature of the CT in question, the energy of the electric dipole of the charge-separated state has to be estimated. Equation 1 gives the free energy of intramolecular charge transfer.[24]

$$\Delta G_{CT} = \Delta E_{redox} + \frac{e^2}{4\pi\varepsilon_0}\left[\left(\frac{1}{r_A}+\frac{1}{r_D}\right)\left(\frac{\varepsilon_r-1}{2\varepsilon_r}\right)-\frac{1}{\rho_{sol}}\left(\frac{\varepsilon_r-1}{2\varepsilon_r+1}\right)-\frac{1}{\rho_{vac}}\right] \quad (1)$$

Here r_D (r_A) is the Born radius for the donor (acceptor), and ρ_{vac} and ρ_{sol} are the lengths of the dipole (often the distance between D and A is simply used) in vacuum and condensed phase, respectively. ΔE_{redox} is measured as the difference between the electrochemical potentials of the reduced and oxidized species. ε_0 is the vacuum permittivity, and ε_r is relative permittivity of the solvent. We estimate r_D (= 3.26 Å) as the radius of a sphere with the molecular volume of the donor (*p*-$(Me_2N)_2C_6H_4$), whereas the previously obtained value for the radius of C_{60} (5.09 Å) is used for r_A.[25] The value of the relative dielectric constant (ε_r) for the solvent mixture without correction for the electrolyte is 18.5.[26] For simplicity we assume ρ_{vac} and ρ_{sol} to be equal (ρ). Figure 2 shows how small changes in ρ results in large changes in the energy of CT in **1**. An upper bound to ρ is the sum of r_D and r_A; however, due to the dipole stabilization terms in eq 1, a smaller value could be expected. Still, even for the lowest reasonable ρ (estimated as 4.5 Å), a positive ΔG_{CT} is found, suggesting that ground state electron transfer does not take place from

(23) Xie, Q.; Ptrez-Cordero, E.; Echegoyen, L. *J. Am. Chem. Soc.* **1992**, *114*, 3978–3980.

(24) (a) Kavarnos, G. J.; Turro, N. J. *Chem. Rev.* **1986**, *86*, 401–449. (b) Chibisov, A. *Usp. Khim.* **1981**, *50*, 1169–1196. (c) Ranger, M.; Rondeau, D.; Leclerc, M. *Macromolecules* **1997**, *30*, 7686–7691.

(25) Dresselhaus, M. S.; Dresselhaus, G. *Annu. Rev. Mater. Sci.* **1995**, *25*, 487–523.

(26) Wohlfarth, C. *Static Dielectric Constants of Pure Liquids and Binary Liquid Mixtures*; Springer: Berlin/Heidelberg, Germany, 2008.

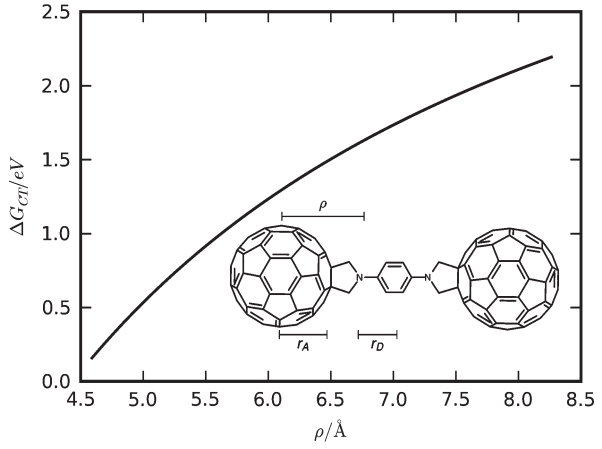

FIGURE 2. The variation of free energy of ground state electron transfer (ΔG_{CT}) with donor−acceptor distance (ρ, size of dipole, see text for details). Data used: $\Delta E_{redox} = 1.31$ eV, $r_D = 3.26$ Å, $r_A = 5.09$ Å, and $\varepsilon_r = 18.5$.

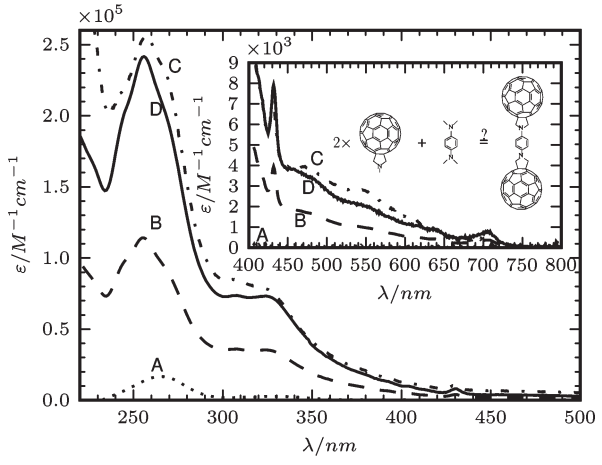

FIGURE 3. UV−vis absorption of (A) *N*,*N*,*N*′,*N*′-tetramethylphenylenediamine, (B) **7**, (C) **1**, and (D) (A) + 2 × (B). The solvent in the main figure was MeCN, and for the insert 1,2-dichlorobenzene (DCB) was used owing to the higher solubility of fullerenes in this solvent. No absorption was observed between 750 and 3000 nm.

the central phenylenediamine to a C_{60} unit. However, absorption to the S1 state of C_{60} provides enough energy (~1.8 eV) to make charge transfer energetically favorable.

Absorption and Emission Spectroscopy. The absorption spectrum of dumbbell **1** in comparison with its molecular constituents is shown in Figure 3. Basically, the absorption spectrum of **1** is the sum of the absorption spectra of *N*,*N*,*N*′,*N*′-tetramethylphenylenediamine and two *N*-methyl fulleropyrrolidines (**7**). Thus, no intramolecular charge-transfer absorption was observed as a result of linking the units together in line with the above-mentioned electrochemical calculations. From the absorption spectra it is also clear that it is possible to excite the C_{60}-part (electron acceptor) of **1** alone. Similar absorption features were observed for the fluorene dumbbell **40**, and also in this system it is possible to electronically excite the compound by using a wavelength above 430 nm (cf., the Supporting Information).

To elucidate in further detail the possibility for electronic communication between the central unit and the C_{60}, we investigated the emission properties of the compounds. Table 2 lists the observed changes in absorption and emission properties of selected compounds. Although the emission quantum yields are small, we first note that the emission quantum yield of the simple fulleropyrollidine **7** is increased by a factor of ca. 4 relative to that of C_{60}.[27] This increase is most likely due to the breaking of symmetry in the C_{60}. The fluorescence quantum yield of compound **14** is very similar to that of **7**. In **19** a more electron-donating anisole group is attached, which is borne out in a minor decrease in the emission. Notably, the emission is significantly quenched for both dumbbells **1** and **40** containing the strong donor units (cf., redox properties, vide supra), as well as for the "half-dumbbell" **43**. The quantum yields were solvent dependent and even smaller in DCB than in CS_2. Thus, for the dumbbells **1** and **40** the quantum yields were ca. halved in DCB (values not listed) relative to in CS_2. On account of the lowering of quantum yields of the dumbbells, as well as the lowering of the quantum yield in the more polar solvent DCB ($\varepsilon_r = 7.5$) compared to CS_2 ($\varepsilon_r = 2.6$), electron transfer from the central unit to the excited C_{60} appears to be a viable quenching mechanism. Table 2 also lists the calculated quenching efficiencies, showing a close to complete quenching of emission in the dumbbell systems.

The electron donor capability of the central phenylenediamine should be altered upon protonation. To investigate electron transfer as a quenching mechanism further in the case of **1**, we studied the change in emission properties upon protonation of the phenylenediamine. For reference compound **7**, the absorption and emission spectra before and after protonation with trifluoroacetic acid are shown in Figure 4a. In this case protonation resulted in blue-shifted absorptions and emission peaks (Table 2). Further, the emission intensity was slightly decreased. The spectra of non-protonated species were recovered by addition of pyridine in large surplus (10 μL) (data not shown).

A similar experiment was performed with dumbbell **1**, and Figure 4b shows the electronic spectra before and after protonation. The absorption increases slightly, while a significant increase in the emission is observed. This is most likely due to destruction of the donor properties by protonation, thus supporting the photoinduced electron transfer as quenching mechanism. In addition, protonation causes a smaller blue-shift for **14** compared to dumbbell **1**, which again experiences a smaller blue-shift compared to **7**. Thus, when the positive charge is more delocalized, the blue-shift is smaller.

Spectroelectrochemistry. Having established that electron transfer takes places upon excitation, but not in the ground state, spectra of oxidized and reduced species were recorded (Table 3), thus resolving the optical transitions of the charged species. In general, electrochemical changes were reversible, and the spectrum of the neutral species could be regenerated by electrolysis. Spectra obtained for **14** are shown in Figure 5, while the complete data are presented in Table 3.

(27) (a) Luo, C.; Fujitsuka, M.; Watanabe, A.; Ito, O.; Gan, L.; Huang, Y.; Huang, C. H. *J. Chem. Soc., Faraday Trans.* **1998**, *94*, 527–532. (b) Wei, X.-W.; Yao, S. D.; Yin, G.; Suo, Z.-Y.; Xu, Z.; Wang, P.; Zhang, W.-J.; Chen, P.; Zhang, Y.; Li, C.-D.; Niu, Y. *Fullerenes, Nanotubes, Carbon Nanostruct.* **2002**, *10*, 137–153.

TABLE 2. Absorption and Emission Data Measured in CS_2 (If Not Otherwise Stated)

compd	absorption λ_{max}/nm ($\varepsilon/10^3$ M^{-1} cm^{-1})	Emission λ_{max}/nm ($\phi/10^{-4}$)[a]	efficiency/%[b]	absorption protonated λ_{max}/nm	emission protonated λ_{max}/nm
C_{60}	435 (3.4); 710 (0.33)	700 (2.6)			
1	435 (7.1); 707 (0.75)[c]	717, 795 (0.3)	97	434, 695	710, 785
7	435 (4.3); 710 (0.38)[c]	719, 795 (10)		432, 693	704, 779
14	435 (5.9); 709 (0.38)[c]	717, 794 (9.1)	9	434, 701	714, 786
17	435 (3.0); 710 (0.30)	715, 794 (4.5−6.5) (0.5−1)[d]	38		
19	408 (5.8); 710 (0.33)	714 (1.5)	85		
40	444 (9.4); 708 (0.95)	717, 795 (0.3)	97		
43	435 (4.9), 709 (0.49)	709 (0.7−1) (0)[d]			

[a]Fluorescence quantum yields are measured for excitation into the electron acceptor moiety (above 430 nm). Uncertainty is ±20%. [b]Calculated as efficiency = $1 - (\phi/\phi_7)$, where ϕ_7 is the quantum yield of **7**. [c]ε is estimated based on the average value of one fulleropyrollidine unit. [d]Solvent: DCB.

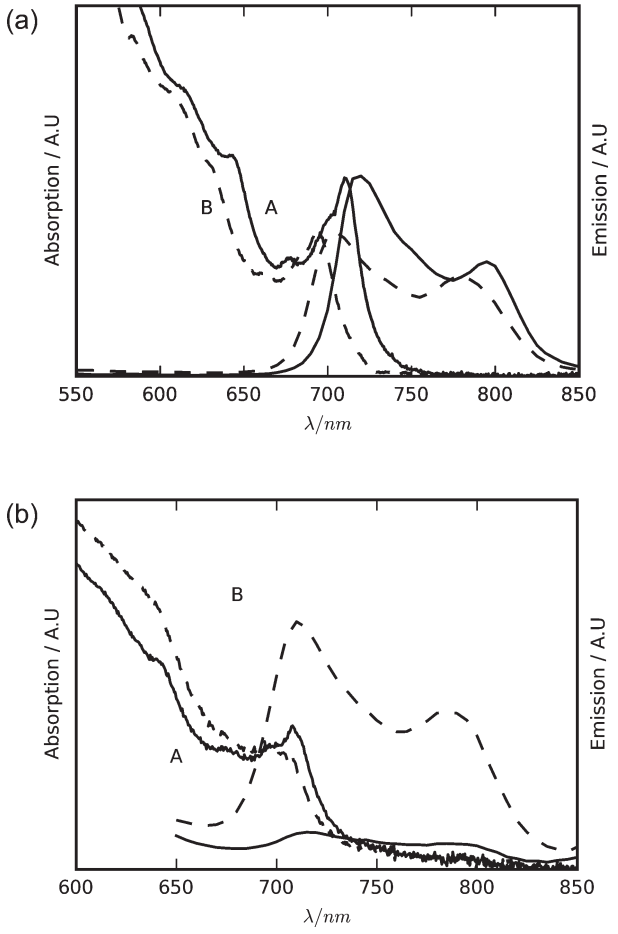

FIGURE 4. (a) Absorption and emission spectra (normalized with respect to the absorption at the excitation wavelength 475 nm) of **7** in CS_2 before (A, solid) and after (B, dashed) protonation. The species (0.14 mM) was protonated by trifluoroacetic acid (ca. 20 mM). (b) Absorption (left) and emission (right) spectra (normalized with respect to the absorption at the excitation wavelength 475 nm) of neutral **1** (A, solid) in CS_2 and protonated **1** (B, dashed). The species (0.03 mM) was protonated by trifluoroacetic acid (ca. 20 mM).

As dumbbell **1** is based on a Würster's blue derivative, which is very prone to oxidation, chemical and electrochemical oxidations of *N*,*N*,*N*′,*N*′-tetramethylphenylenediamine (*p*-$(Me_2N)_2C_6H_4$, Würster's blue) and **1** were compared (Figure 6). To be able to compare directly, the difference spectrum between neutral and oxidized species is shown for both compounds. Both *p*-$(Me_2N)_2C_6H_4$ and **1** show two peaks in the region from 550 to 700 nm. As the spectrum of **1** resembles that of *p*-$(Me_2N)_2C_6H_4$, the charge must be localized on the phenylenediamine bridge of **1**. This also shows that, as in the case of the neutral molecule, no significant molecular orbital mixing between C_{60} (electron acceptor) and the *p*-$(Me_2N)_2C_6H_4$ (electron donor) is observed in the charged state (in accordance with calculations, vide infra).

Quantum Chemical Calculations. We have first analyzed the geometric and electronic properties of the isolated dumbbell molecule **1** followed by the properties of this molecule in a junction between gold electrodes in order to assess and explain the possibility of electron transmission through it.

Isolated Molecules. C_{60} has two types of bonds: those shared by two hexagons denoted [66] and by a hexagon and a pentagon denoted [56]. B3LYP/6-31g** geometry optimization yields the [66] length equal to 1.396 Å and that of [56] equal to 1.454 Å, in very good agreement with their experimental values of 1.401 and 1.458 Å.[28] Functionalization with pyrrolidine by the Prato reaction is an addition to a [66] double bond. The geometry optimization shows that the effect of this addition is rather localized by conserving the overall structure of C_{60} though with pronounced local geometric distortions. In fulleropyrrolidine, the substituted [66] bond length increases to 1.616 Å, and that of the four adjacent [56] bonds to 1.534 Å. Practically the same values are found in **1**: 1.610 and 1.533 Å, respectively. In the pyrrolidine ring of **1**, the C−C bond length is 1.558 Å, and that of C−N is 1.454 Å. The pyrrolidine−phenylene N−C bond length is 1.409 Å. Such long bond lengths already suggest that conjugation of C_{60} with benzene is practically nonexistent.

The pyrrolidine ring is nonplanar, with at least one atom out-of-plane. While different potential minima are found for free pyrrolidine,[29] only the one with its four carbons in-plane and nitrogen out-of-plane is found by geometry optimization for **1**, whatever the initial geometry. The pyramidality of the pyrrolidine nitrogen in **1** is relatively low compared to that of aliphatic amines: the sum of its three bond angles is $(2 \times 119.4°) + 106.9° = 345.7°$. The NC2C3C4 dihedral angle (all four atoms belonging to pyrrolidine) is 23.2°, and the C(Ph)NC2C5 dihedral angle is 139.6°. Note that the C(Ph)NC2C3 dihedral angle is 180° so that the phenylene is parallel to the pyrrolidine carbons, standing upright with respect to the C_{60} distorted sphere. This minimum energy

(28) Andreoni, W. *Annu. Rev. Phys. Chem.* **1998**, *49*, 405–439.
(29) (a) Han, S. J.; Kang, Y. K. *THEOCHEM* **1996**, *369*, 157–165. (b) El-Gogary, T. M.; Soliman, M. S. *Spectrochim. Acta, Part A* **2001**, *57*, 2647–2657.

TABLE 3. Selected Absorption Data (λ_{max}/nm) and Molar Absorptivities (in Parentheses) ($\varepsilon/10^3$ M^{-1} cm^{-1}) of Charged Species in Comparison to Those of C_{60} Measured by Spectroelectrochemistry[a]

compd	anion	dianion	trianion	cation	dication
C_{60}	1078 (12.3)	838 (8.1), 951 (17)			
p-$(Me_2N)_2C_6H_4$[b]				565 (10.0), 612 (9.5)	
1				584 (11.3), 628 (10.6)	
7	995 (6.9)	864 (8.1)			
14	997 (7.7)	731 (8.7), 865 (12.7)	684(9.7), 875(10.5)		
17	611 (15.8), 997 (12.3)	731 (12.7), 868 (19.2)			
19	998 (7.3)	733 (4.1), 863 (5.0)			
43	998 (5.5)	733 (6.9), 868 (9.9)		460 (10.8), 811 (4.8), 908 (8.3)	462 (12.7), 821 (6.0), 924 (9.2)

[a]Molar absorptivity of peaks is relative to the neutral species, where concentrations have been estimated using the peak height at 435 nm. Only absorption maxima above 500 nm are listed. Solvent: MeCN:DCB (1:2) + 0.133 M Bu_4NPF_6. [b]Measured in MeCN + 0.1 M Bu_4NPF_6.

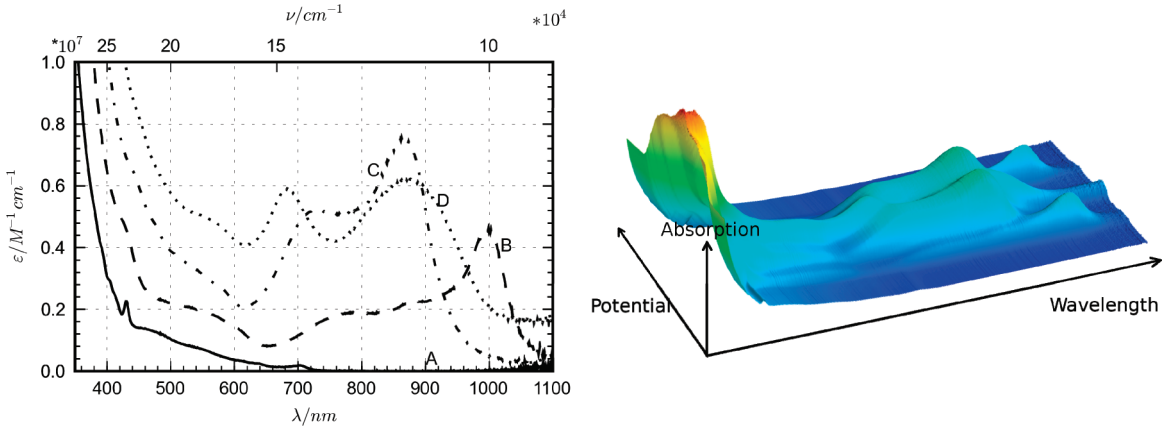

FIGURE 5. Spectroelectrochemical reduction of **14** in MeCN: (A, solid) neutral, (B, dashed) anion, (C, dash-dot) dianion, and (D, dotted) trianion. The right-hand side shows how the absorption changes reversibly through the different charged states. The potential was swept very slowly ($\approx 10^{-4}$ V/s) to −2.0 V, while recording the absorption spectra. Lines A, B, C, and D are the first to fourth plateau in absorbance vs potential. When sweeping back from −2.0 V the same spectra were obtained.

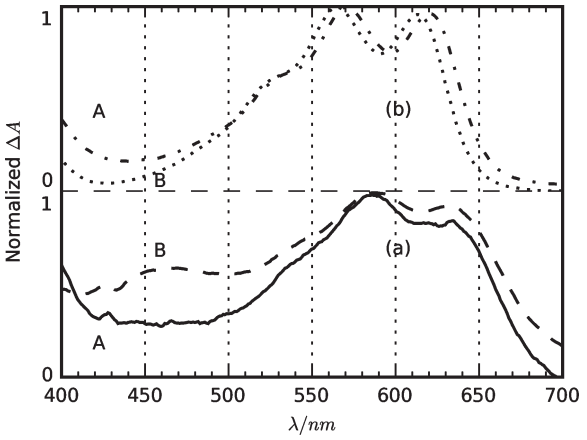

FIGURE 6. Oxidation difference spectra: (a) chemical oxidation, (b) spectroelectrochemical oxidation of (A) *p*-$(Me_2N)_2C_6H_4$ in MeCN and (B) **1** in MeCN:DCB (1:2). The spectrum of the neutral species was subtracted from the spectrum of the radical cation after normalization.

conformation practically excludes any possibility of through-space conjugation between the fullerene and phenylene units.

The frontier energy levels of C_{60} have been computed at the B3LYP/6-31g** level; this gives a 5-fold degenerate HOMO at −5.98 eV and a 3-fold degenerate LUMO at −3.22 eV, which is a HOMO−LUMO gap of 2.76 eV. The experimental ionization energy (IE) and electron affinity (EA) values are around 7.6 and 2.6 eV,[30] which yields a gap around 5.0 eV. The estimates based on the B3LYP orbital energies within a one-electron picture are rather far from reality; however, the vertical IE and EA estimates based on total energy differences between the neutral and ionized states are much more satisfactory, namely, 7.15 and 1.99 eV, respectively; this leads to a gap of 5.16 eV, in good agreement with the experimental value. The nuclear relaxation energies for the cation and anion of C_{60} are computed to be rather small, 5.9 and 63.6 meV, respectively. Indeed, C_{60} is notorious for very low electron−phonon coupling and reorganization energy among aromatic hydrocarbons.[31] Functionalization by pyrrolidine at a [66] bond lifts the degeneracy in the MOs. In fulleropyrrolidine, the HOMO quintet and the LUMO triplet are split into 5 occupied and 3 vacant levels with the B3LYP eigenenergies (−6.20, −5.83, −5.78, −5.77, −5.62) and (−3.07, −2.97, −2.73) eV, whose shift and splitting with respect to fully symmetric C_{60} are very similar to those previously reported.[32] In dumbbell **1**, there are 6 lowest-lying unoccupied MOs originating from the two sets of triply degenerate LUMOs of C_{60}, without any contribution from phenylenediamine, coming in pairs with the B3LYP-calculated energies of −3.18, −3.07, and −2.83 eV. The degeneracy for each fullerene is lifted upon substitution but the

(30) NIST Chemistry Webbook.

(31) (a) Imahori, H.; Hagiwara, K.; Akiyama, T.; Aoki, M.; Taniguchi, S.; Okada, T.; Shirakawa, M.; Sakata, Y. *Chem. Phys. Lett.* **1996**, *263*, 545–550. (b) Devos, A.; Lannoo, M. *Phys. Rev. B* **1998**, *58*, 8236.

(32) Hirsch, A. *Top. Curr. Chem.* **1999**, *199*, 1–65.

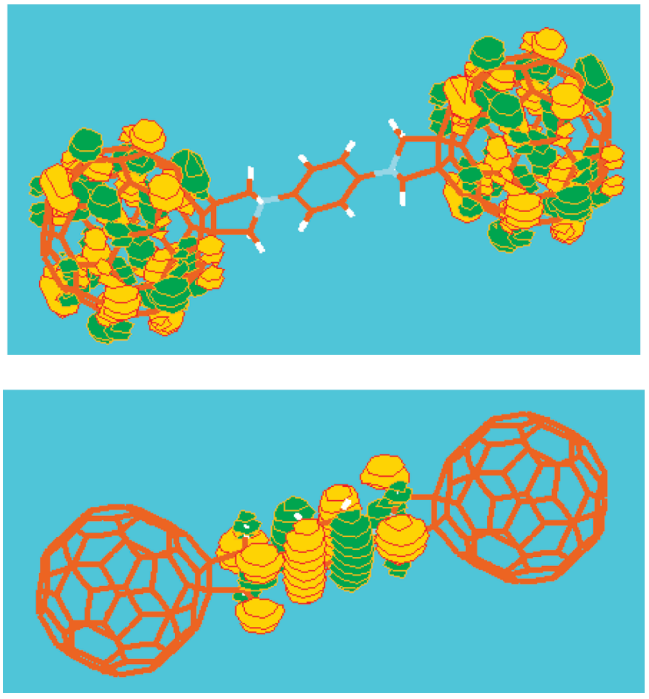

FIGURE 7. Frontier orbitals of **1**: HOMO (bottom) and LUMO (top, one of the degenerate pair).

splitting in the pairs is negligible since there is virtually no coupling between the fullerenes. The HOMO of **1** is centered on the phenylenediamine unit (Figure 7) and is found at −5.10 eV; it is followed by 5 pairs of fullerene MOs at −5.72, −5.87, −5.88, −5.93, −6.30 eV originating from the 10 degenerate HOMOs of the two fullerenes. Again, there is virtually no splitting in the pairs of fullerene MOs.

The vertical IE and EA calculated from total energy differences are 6.28 and 2.40 eV, respectively. The increase in EA can be explained primarily by anion stabilization due to charge sharing between the two fullerenes by symmetry in a free molecule (such equal partitioning is hardly robust in a realistic environment). On the other hand, the significantly decreased IE is due to electron abstraction from the phenylenediamine donor. For comparison, experimental IE of tetramethylphenylenediamine is 6.2 eV.[30] The relaxation energy of the positive and negative ion is 366 and 34 meV, respectively. The relaxation energy in the cation, which is much higher than the typical value for the fullerene, is due to the positive charge localization on the phenylenediamine bridge.

Molecular Junctions. We now turn to the results of the electron transport calculations. The geometry of the junctions is shown in Figure 8. To assess the conductance through the triad **1**, it is more relevant to compare it with that of fullerene under the same conditions (Figure 9). With C_{60}, there are three transmission peaks within 2 eV from the Fermi level at zero bias. Transmission peaks are easily identified with the isolated molecule MOs calculated with the same method and basis set. Their intensity is higher than one (maximum probability per orbital) because of degeneracy. It is the C_{60} LUMO that is closely aligned with the Fermi level and is therefore primarily responsible for transmission at low bias. We note that the HOMO−LUMO transport gap at this level of theory is 1.63 eV, which is too low for an isolated molecule but most reasonable for a molecule in a

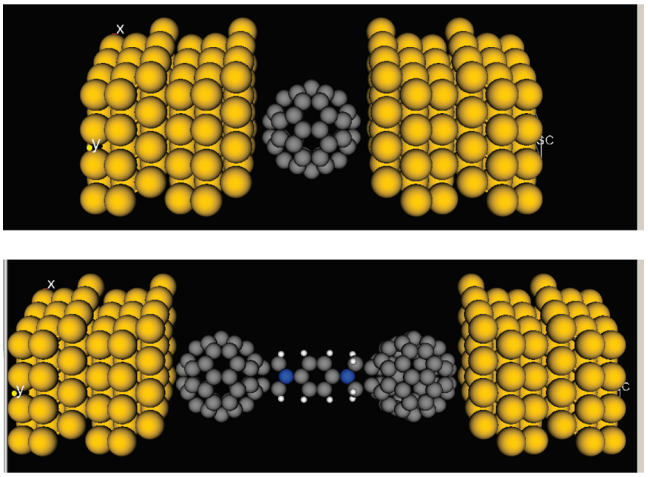

FIGURE 8. Geometry of the junctions including C_{60} (top) and **1** (bottom) (explained in more detail in the Theoretical Methodology section).

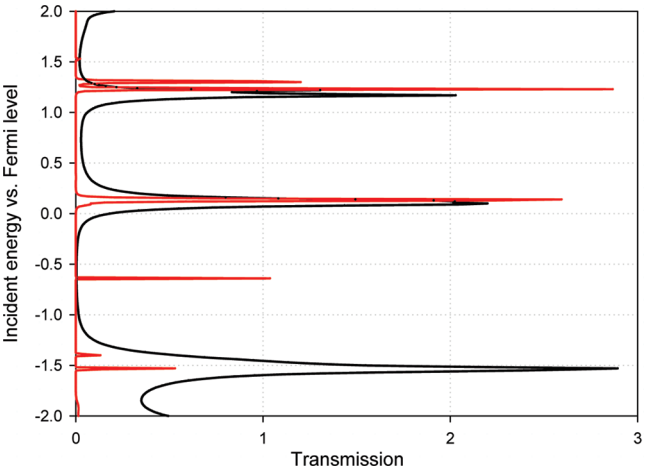

FIGURE 9. Transmission under zero bias: black, C_{60}; red, **1** (transmission multiplied by 20).

medium. The transport gap is renormalized to 2.3 eV for C_{60} monolayer adsorbed on Au(111) according to recent experimental data,[6d] and we expect even stronger renormalization for a molecule between two metal surfaces. However, the quality of the HOMO−LUMO gap prediction is relatively unimportant in the present context since the transmission is clearly dominated by the LUMO, pinned at the Fermi level following partial electron transfer from the metal.

Application of a bias drives the system out of equilibrium and opens the transmission window between the Fermi levels of the left and right electrodes, which allows current flowing through the junction (Figure 10). Under bias, the shape of the transmission spectrum does not change. The low-energy edge of the LUMO transmission peak remains pinned to the higher Fermi level: since the LUMO remains only partially occupied, a part of its peak is left out of the transmission window. An increasing part of the peak is gradually entering the transmission window leading to a current increase with bias.

Turning now to the transmission spectrum of **1** (Figure 11), we note first that there are still peaks present at the energies

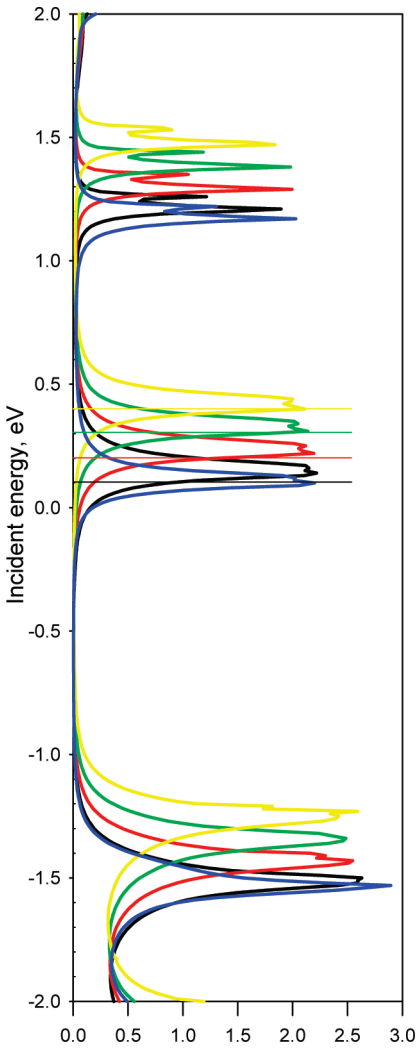

FIGURE 10. Transmission of C_{60} under bias: 0.0 (blue), 0.2 (black), 0.4 (red), 0.6 (green), and 0.8 V (yellow). The horizontal line of each color shows the position of the higher Fermi level (that of the negative electrode, half-bias from the origin).

corresponding to those of the C_{60} HOMO (now HOMO-1 of the entire triad), LUMO, and LUMO+1. Again, it is the LUMO peak that is most closely aligned to the Fermi level. There is an additional peak at −0.64 eV originating from the HOMO of the phenylenediamine bridge, which is now the HOMO of the triad molecule, as discussed above. However, the intensity and width of all transmission peaks for **1** decrease drastically. The most likely reason is the insufficient conjugation throughout the molecule. For the C_{60} orbitals, the overlap of each fullerene with its electrode is still ensured, but between fullerenes, there are no available MOs on the bridge at the corresponding energy, thus reducing drastically the probability of transmission from one electrode to the other through the molecule. When a bias is applied, the transmission spectrum of **1** undergoes spectacular changes unlike that of C_{60}, which remains qualitatively the same.

At zero bias, the left and right fullerenes of **1** positioned in a symmetric junction are in the same environment. Consequently, all MOs of **1** and transmission peaks originating from C_{60} come as degenerate pairs: the symmetric and antisymmetric linear combinations of the orbitals of the left and right C_{60} counterparts have the same energy as there is no overlap between them. Note that the localization of the split MOs at the opposite fullerenes comes at no price in energy, since it does not require any bond breaking either inside the molecule or between the molecule and the metal. Therefore, there is no threshold field to reach this situation. This differs from fullerene in a junction, for which a similar localization at the opposite sides of the same fullerene sphere could be envisaged only at some high, probably unattainable, bias. The electric field induced by bias lifts this degeneracy: the MOs of **1** become localized on one of the fullerenes, and their energies increase practically linearly with bias on one side and decrease on the other side. The energy of the orbitals localized on the bridge is practically independent of bias since they are positioned symmetrically with respect to the electrodes. The deviations from linearity (for C_{60}) and constancy (for the bridge) are due to the polarization of the orbitals, which is a second-order effect with respect to the electric field (square dependence) and therefore becomes efficient at high bias. These considerations help us in deciphering the evolution of the transmission spectrum of **1** under bias. The peaks originating from the C_{60} orbitals, in particular the most relevant LUMO peak, have their degeneracy lifted when bias is applied and their position on the energy scale evolves quasilinearly, with deviations of such a linearity manifested at higher bias. The shift in the position of the C_{60}-based transmission peaks is accompanied by a drastic decrease in their intensity. Indeed, an electron from an orbital now localized on one fullerene has to tunnel a much longer way (equal to the length of the bridge and the opposite fullerene) to the other electrode, practically through-space since there are no states with the appropriate energy over the bridge. A superexchange mechanism[33] is not playing any role in our system as there is no overlap between the MOs localized on C_{60} and on the phenylenediamine bridge. On the contrary, the position of the transmission peak of **1** originating from its HOMO localized over the bridge remains practically constant and its intensity is much less affected by bias. However, this HOMO-derived peak is of little use for conductance as it is far from the transmission window at reasonable bias and narrow due to lack of overlap with the electrodes through the other parts of the molecule.

In all, this theoretical study demonstrates that weak coupling between the parts of our molecular triad, in spite of good coupling of the terminal fullerenes to metal electrodes, is detrimental for electronic transmission in the coherent regime at zero bias when compared to fullerene; moreover, there is a more serious collapse of conductance under bias due to electric-field-induced localization of molecular orbitals. To further support this conclusion, we refer to the experimental study in ref 8, where a typical conductance in the range from 0.01 to 0.1 G_0 was registered for C_{60}, while for **1** values around 3×10^{-4} G_0 were obtained under the same experimental conditions. We have thus reached the conclusion of insufficient electronic coupling between the fulleropyrrolidin-1-yl and bridge moieties to achieve coherent transport.

(33) (a) Sun, M.; Chen, Y.; Song, P.; Ma, F. *Chem. Phys. Lett.* **2005**, *413*, 110–117. (b) Sun, M.; Song, P.; Chen, Y.; Ma, F. *Chem. Phys. Lett.* **2005**, *416*, 94–99.

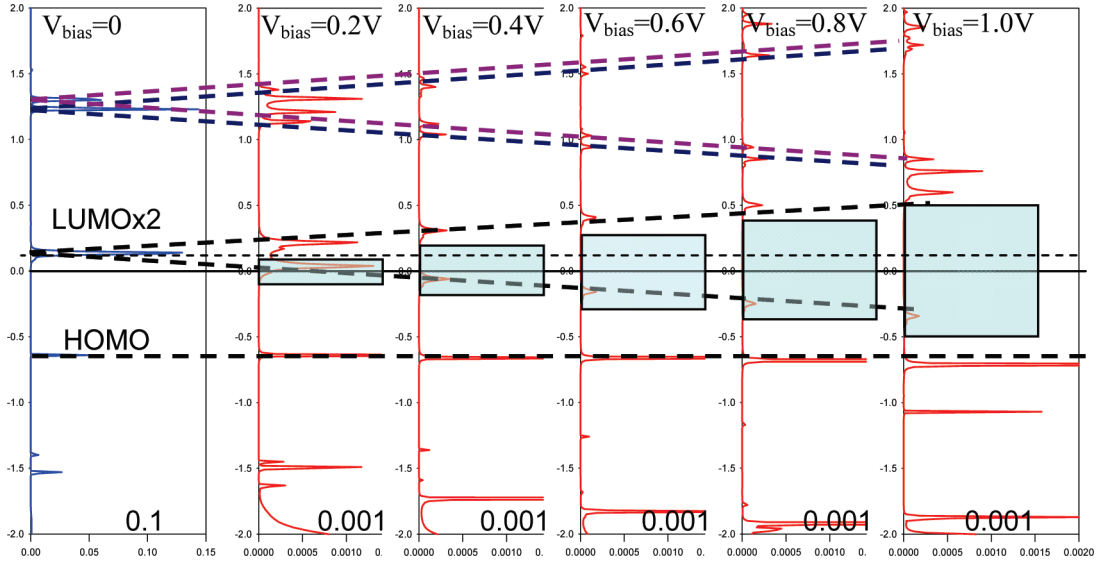

FIGURE 11. Evolution of the transmission spectrum of **1** under bias.

SCHEME 11. Modified Prato Reactions

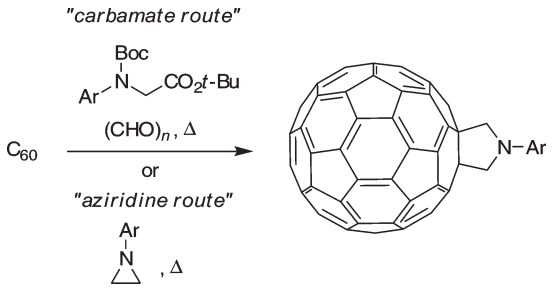

Conclusions

In conclusion, we have developed synthetic protocols for novel C_{60} end-capped molecular wires incorporating a central donor unit derived from phenylenediamine, fluorenediamine, and different anilines. The compounds were prepared by using different variations of the Prato reaction. In particular, we have found that the cycloaddition can be accomplished from a simple mono- and diaziridine precursor derived from aniline and fluorenediamine, respectively, with no substituent groups required at the aziridine carbon atoms. In contrast, a 2-fold Prato reaction from a diaziridine derived from phenylenediamine failed. Nevertheless, a selection of useful aniline building blocks for further scaffolding was developed. In another protocol, the corresponding carbamate (Boc group) was *N*-alkylated with *tert*-butyl bromoacetate to provide a stable compound that could be directly used for the Prato reaction with C_{60} and paraformaldehyde as both the carbamate and *tert*-butyl ester groups were removed in situ under the reaction conditions. The advantage of both the "aziridine" and "carbamate" protocols is the ready purification of the immediate precursor for the Prato reaction. The methods presented in Scheme 1 can now be extended to those shown in Scheme 11.

The compounds were subjected to detailed physicochemical studies. While little communication between the central donor unit and C_{60} end-groups was observed in the ground state, the units communicate in the excited state. Thus, the C_{60} fluorescence is partly quenched by the phenylenediamine donor unit via an electron transfer mechanism. For dumbbell **1** in a single-molecule junction, we predict a significant decrease in coherent transmission, in comparison to C_{60}, at zero bias followed by a further collapse of conductance under bias due to electric-field-induced localization of essential molecular orbitals at the opposite sides of the molecule. Though C_{60} remains an appropriate anchor group in a functionalized fullerene, the absence of conjugation between the parts of our molecular dumbbell triad is detrimental for electronic transmission in the coherent regime. However, the well-defined symmetric tunneling barrier between the two C_{60} units and the bridge, which allows each constituent part of the triad to conserve its identity, probably makes C_{60} end-capped "molecular wires" suited for electron transport in molecular junction in the weak coupling (Coulomb blockade) regime and dependent on the electronic properties of the bridge. The dumbbell design is thus well-suited for achieving structure−property relationships.

Experimental Section and Theoretical Methodology

Electrochemistry. The compounds were dissolved in DCB (2 mL) to obtain millimolar concentrations after 0.4 M tetrabutylammonium hexafluorophosphate ($TBAPF_6$) in MeCN (1 mL) was added, yielding a final $TBAPF_6$ concentration of 0.13 M. Ag/Ag^+ was used as reference electrode. Electrolyte solution was added to a compartment separated by a porous tip containing a Ag wire. As counter electrode a platinum wire was used. All potentials are reported against ferrocene(II/III) measured under the same conditions. A minimum of four sweep rates were used in cyclic voltammetry (CV) experiments to ensure electrochemical reversibility. Typical sweep rates were between 1 and 0.02 V/s. In square-wave voltammetry (SWV) experiments a minimum of four frequencies between 100 and 1 Hz were used.

Absorption Spectroscopy. Solvent absorption scattered light was corrected for when necessary. Calculated extinction coefficients have uncertainties estimated to 10% due to limited sample quantities.

Emission Spectroscopy. Fluorescence measurements were carried out with a 450 W xenon lamp. Quantum yields were

measured at low concentrations to ensure linearity with at least 3 different concentrations for each sample using C_{60} in DCB (3.0×10^{-4} M) and CS_2 (2.6×10^{-4} M) as references.[34] Uncertainties are estimated to 20%.

Spectroelectrochemistry. A thin (~1 mm) glass spectroelectrochemical cell was used in the spectrophotometer. A platinum grid was used as working electrode, and Ag/Ag^+ was used as reference electrode. The counter electrode (platinum wire) was placed in a compartment separated by a porous membrane. The potential was swept very slowly ($\approx 10^{-4}$ V/s) through the potentials of interest in a cyclic manner while recording the absorption spectra. Reversibility of the spectra was ensured, and charged species was identified as plateau in the change of absorption. The spectra may contain a mixture of solution and interface components.

Quantum Chemical Calculations. The geometry of the isolated molecules (neutral and charged **1** and its fragments) was fully optimized at the hybrid DFT B3LYP/6-31g** level, based on previous studies demonstrating that B3LYP is very successful for the description of fullerenes, even with a small basis set.[35] These calculations were performed with the Gaussian 03 program.[36] Transmission of molecular junctions was studied by the NEGF method[37] as implemented in the ATK2008 program[38] with the LDA DFT functional. LDA is notorious for severely underestimating the HOMO−LUMO gaps of free molecules. However, by this strong underestimation, it implicitly takes into account the renormalization of molecular levels in the vicinity of metal. For this reason, LDA description of the C_{60} transmission spectrum in molecular junctions was in excellent agreement with the STS spectroscopic data.[6b] The basis set used was SZP for Au and DZP for the organic molecules. The metal electrode is Au(111); the unit cell size was fixed at 4×4 Au laterally, after having verified with C_{60} that increasing it to 5×5 does not alter the results noticeably. The central region includes 3 metal layers. The *k*-point sampling is $3 \times 3 \times 50$ Monkhorst−Pack.

It was not our objective in this study to determine the optimum adsorption geometry for C_{60} and dumbbell **1** in an ideal junction, which could be important if we aimed at precise absolute transmission values for such an idealized situation. We take it for granted that C_{60} and **1** are chemisorbed in the same way, as the functionalization leaves the opposite side of C_{60} undisturbed. It should also be taken into account that molecular junctions are dynamic structures. We aim therefore at comparing the transmission of C_{60} and dumbbell **1** at the same reasonable adsorption geometry. Various adsorption geometries of C_{60} on Au have been considered theoretically and observed in experiments, as there is no single predominant molecular orientation on this surface.[39] In this work, the arrangement is with C_{60} adsorbed on-top with its [66] bond (in the case of **1**, it is the bond opposite to that functionalized with pyrrolidine) at the distance to Au kept at 2.75 Å;[6b,40] the free-molecule geometry was not reoptimized in the junction.

Synthesis. For reactions carried out under inert atmosphere the glassware was oven-dried at 120 °C before use or heated under evacuation and flushed with argon. All reagents were purchased from major suppliers and used without further purification unless otherwise noted. All solvents were analytically grade and dried when necessary over either 3 or 4 Å activated molecular sieves. Water content was determined to be less than 20 ppm by Karl Fischer titration. Thin layer chromatography (TLC) was carried out on commercially available precoated plates. Dry column vacuum chromatography (DCVC) was performed according to a published procedure.[41] Melting points were measured on a microscope hot stage melting point apparatus or a silicone oil bath apparatus and are uncorrected. ^{1}H, ^{13}C, APT, DEPT, HMQC, HMBC, and NOE NMR spectra were recorded on 300, 400, or 500 MHz spectrometers with use of an internal deuterium lock. Solvent residual chemical shifts were used as internal standards when assigning NMR spectra (δ_H: $CDCl_3$ 7.26 ppm, DMSO-d_6 2.50 ppm; δ_C: $CDCl_3$ 77.0 ppm, DMSO-d_6 39.4 ppm). Infrared spectra were recorded with a KBr pellet (ca. 1 mg of compound and ca. 100 mg of KBr).

1,4-Bis(fullero[*c*]pyrrolidin-1-yl)benzene (1). Method 1. *N*,*N*′-(1,4-Phenylene)bis(glycine) (30 mg, 0.13 mmol) and paraformaldehyde (20 mg, 0.67 mmol) were suspended in 1,2-dichlorobenzene (10 mL) and sonicated for 10 min. C_{60} (1.0 g, 1.4 mmol) was then added together with 1,2-dichlorobenzene (50 mL), and the mixture was heated to reflux for 18 h. The product together with some remaining C_{60} was precipitated by the addition of heptane at rt. The precipitate was subjected to Soxhlet extraction with use of 1,2-dichlorobenzene for 18 h. This procedure (precipitation by heptane followed by Soxhlet extraction) was repeated a total of three times, after which the Soxhlet filtrate was no longer purple from C_{60}, but brown from the fulleropyrrolidine product. The product was then purified by dry column chromatography (SiO_2, decalin → 30% 1,2-dichlorobenzene in decalin). A total of three column chromatographic purifications were necessary to obtain a pure product (9 mg, 5%) as a brown powder (of very limited solubility) that crystallized in small dark brown leaf-like crystals from 1,2-dichlorobenzene upon standing. IR: 2924 (w), 2854 (w), 2798 (w), 1614 (m), 1466 (s, br), 1150 (s) cm^{-1}; ^{1}H NMR (400 MHz, CS_2/acetone-d_6) δ 7.51 (s, 4 H), 5.26 (s, 8 H) ppm; ^{13}C NMR, not soluble enough; MS (MALDI-TOF, negative mode) *m*/*z* 1601 [M + H$^-$].

Method 2. C_{60} (500 mg, 0.69 mmol) and **6** (91 mg, 0.17 mmol) were dissolved in 1-chloronaphthalene (13 mL), and the solution was sonicated under a stream of argon for 10 min. Then *p*-toluenesulfonic acid (ca. 1 mg) and paraformaldehyde (100 mg, 3.33 mmol) were added, and the mixture was heated to reflux for 2 h. The product was precipitated by the addition of heptane, filtered off on silica, washed with heptane, and redissolved in 1,2-dichlorobenzene. Excess C_{60} was removed on a silica column (by continuous extraction with cyclohexane as eluent and refluxing it with a Soxhlet setup). Finally, the residue was purified by column chromatography (SiO_2, 30% 1,2-dichlorobenzene in decalin) to yield **1** as a brown powder (12 mg, 5%).

***tert*-Butyl 1,4-Phenylenedicarbamate (5).** 1,4-Phenylenediamine (2.50 g, 23 mmol) was dissolved in CH_2Cl_2 (200 mL) and NEt_3 (7 mL). Then Boc_2O (11.0 g, 48 mmol) was added, and the solution was stirred under an atmosphere of nitrogen at rt overnight. The product was isolated by filtration and recrystallized from hot isopropyl alcohol to yield **5** as a white solid (3.63 g, 51%). IR 3360 (m), 2982 (m), 2935 (w), 1698 (s), 1534 (s), 1160 (s) cm^{-1}; ^{1}H NMR (300 MHz, DMSO-d_6) δ 9.12 (s, 2 H), 7.28 (s, 4 H), 1.44 (s, 18 H) ppm; ^{13}C NMR (75 MHz, DMSO-d_6) δ 153.5, 134.7, 119.3, 79.4, 28.8 ppm; MS (ESI) *m*/*z* 331 [M + Na$^+$]. Anal. Calcd for $C_{16}H_{24}N_2O_4$: C 62.32, H 7.84, N 9.08. Found: C 62.26, H 7.93, N 9.22.

***tert*-Butyl 2,2′-[1,4-Phenylenebis(*tert*-butoxycarbonylazanediyl)]-diacetate (6).** Compound **5** (1.00 g, 3.24 mmol) was dissolved in dry and deoxygenated DMF (30 mL) and the solution was cooled to 0 °C. Then NaH (130 mg, 60 wt % in oil, 3.24 mmol)

(34) Ma, B.; Sun, Y. *J. Chem. Soc., Perkin Trans. 2* **1996**, 2157–2162.
(35) Zandler, M. E.; D'Souza, F. *C. R. Chim.* **2006**, *9*, 960–981.
(36) *Gaussian 03*, Revision C.02; Frisch, M. J.; et al. Gaussian, Inc., Wallingford, CT, 2004.
(37) Brandbyge, M.; Mozos, J.-L.; Ordejón, P.; Taylor, J.; Stokbro, K. *Phys. Rev. B* **2002**, *65*, 165401.
(38) ATK, Version 2008.10, quantumwise.com.
(39) Rogero, C.; Pascual, J. I.; Gómez-Herrero, J.; Baró, A. M. *J. Chem. Phys.* **2002**, *116*, 832–836.
(40) (a) Perez-Jimenez, A. J.; Palacios, J. J.; Louis, E.; SanFabian, E.; Verges, J. A. *ChemPhysChem* **2003**, *4*, 388–392. (b) Stadler, R.; Kubatkin, S.; Bjørnholm, T. *Nanotechnology* **2007**, *18*, 165501.
(41) Rosenbohm, C.; Pedersen, D. S. *Synthesis* **2001**, 2431–2434.

was added, and the suspension was stirred for 10 min, after which *tert*-butyl bromoacetate (480 μL, 634 mg, 3.24 mmol) was added. The mixture was allowed to reach rt and was then stirred for 60 min. Then it was again cooled to 0 °C and the same procedure was followed in adding another portion of NaH and *tert*-butyl bromoacetate. The mixture was stirred overnight at rt and quenched with brine. The product was extracted with heptane/EtOAc (50:50). The crude solution was filtered through a short plug of silica, evaporated to dryness, and was then recrystallized from hot isopropyl alcohol to yield **6** as a white powder (1320 mg, 76%). IR 2980 (m), 2934 (w), 1742 (s), 1707 (s), 1383 (s), 1366 (s), 1232 (s), 1157 (s) cm^{-1}; ^1H NMR (300 MHz, $CDCl_3$) δ 7.23 (s, 4 H), 4.13 (s, 4 H), 1.47/1.44 (2s, 36 H) ppm; ^{13}C NMR (75 MHz, $CDCl_3$) δ 169.1, 154.6, 141.0, 126.9, 81.9, 81.1, 53.2, 28.4, 28.3 ppm; MS (ESI) *m*/*z* 559 [M + Na^+]. Anal. Calcd for $C_{28}H_{44}N_2O_8$: C 62.67, H 8.26, N 5.22. Found: C 62.70, H 8.47, N 5.20.

2-Chloro-*N* -(4-octylphenyl)ethanamide (11). Compound **10** (1.08 g, 5.25 mmol) and K_2CO_3 (1 g, 7 mmol) were added to DMF (25 mL) at 0 °C. Chloroacetyl chloride (500 μL) was added dropwise during 30 min, and the reaction mixture was stirred overnight while being allowed to warm to rt. The product was precipitated by the addition of brine (250 mL), dried, and recrystallized from hot MeOH to give **11** as a white powder (1.13 g, 76%). Mp 119−120 °C; IR 3430 (m), 3278 (m), 2958 (m), 2918 (s), 2848 (s), 1672 (s), 1615 (s), 1555 (m), 1515 (m) cm^{-1}; ^1H NMR (300 MHz, $CDCl_3$) δ 8.10 (s, 1H), 7.36 (d, J = 8.4 Hz, 2H), 7.09 (d, J = 8.4 Hz, 2H), 4.11 (s, 2H), 2.51 (m, 2H), 1.52 (m, 2H), 1.30−1.16 (br, 10H), 0.81 (t, J = 6.8 Hz, 3H) ppm; ^{13}C NMR (75 MHz, $CDCl_3$) δ 163.8, 140.4, 134.4, 129.2, 120.4, 43.1, 35.6, 32.1, 31.7, 29.7, 29.5 (2 signals), 22.9, 14.3 ppm. Anal. Calcd for $C_{16}H_{24}ClNO$: C 68.19, H 8.58, N 4.97. Found: C 68.16, H 8.37, N 4.99.

***N*-(2-Chloroethyl)-4-octylaniline (12).** Compound **11** (1.0 g, 3.5 mmol) was dissolved in THF (200 mL) and cooled to 0 °C. Borane−dimethyl sulfide complex (4 mL, 40 mmol) was added with stirring under argon. The reaction mixture was stirred at rt overnight, then quenched by careful addition of water (10 mL) and stirred until no more gas evolved. The solution was then concentrated in vacuo to ca. 50 mL and diluted with water (100 mL). The product was extracted with heptane (3 × 25 mL); the combined organic phases were washed with water (50 mL), dried (Na_2SO_4), and concentrated in vacuo to a colorless oil that was purified by column chromatography (SiO_2, 10% EtOAc in heptane) to afford the product **12** (780 mg, 82%). ^1H NMR (300 MHz, $CDCl_3$) δ 7.01 (d, J = 4.5 Hz, 2H), 6.58 (d, J = 4.5 Hz, 2H), 3.96 (br, 1H), 3.71 (t, J = 5.9 Hz, 2H), 3.48 (t, J = 5.9 Hz, 2H), 2.50 (t, J = 7.7 Hz, 2H), 1.55 (m, 2H), 1.40−1.15 (m, 10H), 0.88 (t, J = 6.8 Hz, 3H) ppm; ^{13}C NMR (75 MHz, $CDCl_3$) δ 145.1, 133.1, 129.5, 113.6, 46.0, 43.8, 35.3, 32.1, 32.0, 29.7, 29.5, 29.5, 22.9, 14.3 ppm.

1-(4-Octylphenyl)aziridine (13). Compound **12** (500 mg, 1.87 mmol) was dissolved in DMSO (5 mL) and then transferred slowly to a suspension of NaH (100 mg, 60 wt % in oil, 2.5 mmol) in DMSO (5 mL). After 30 min, the solution was heated to 40 °C and stirred under argon for 4 h. The reaction was then cooled and quenched with brine, and then the product was extracted with heptane (3 × 20 mL), dried (Na_2SO_4), and purified by column chromatography (SiO_2, 20% EtOAc in heptane) to yield **13** as a colorless oil (210 mg, 49%). IR 3059 (m), 3024 (m), 2955 (s), 2854 (s), 1510 (s), 1319 (s), 1163 (m), 905 (m), 838 (m) cm^{-1}; ^1H NMR (300 MHz, $CDCl_3$) δ 7.05 (d, J = 8.3 Hz, 2H), 6.93 (d, J = 8.3 Hz, 2H), 2.52 (t, J = 7.7 Hz, 2H), 2.07 (s, 4H), 1.67−1.48 (m, 2H), 1.43−1.17 (m, 10H), 0.88 (t, J = 6.7 Hz, 3H) ppm; ^{13}C NMR (75 MHz, $CDCl_3$) δ 153.0, 137.1, 129.0, 121.0, 35.5, 32.1, 31.9, 29.7, 29.6, 29.5, 27.8, 22.9, 14.3 ppm; MS (EI) *m*/*z* 231 [M^+], 132 [M − C_7H_{15}]$^+$; HR-MS (ESI) *m*/*z* 232.2094 (M + H^+ calcd for $C_{16}H_{26}N$ 232.2065).

1-(4-Octylphenyl)fulleropyrrolidine (14). Method 1. Compound **13** (30.2 mg, 0.13 mmol) and C_{60} (500 mg, 0.69 mmol) were dissolved in 1,2-dichlorobenzene (5 mL) in a sealed glass tube. The reaction was heated to 200 °C overnight and was then cooled and evaporated to dryness at reduced pressure. The product was purified by repeated column chromatography (SiO_2, 25% *o*-xylene in cyclohexane) and finally precipitated from *o*-xylene by the addition of MeOH to yield the product **14** as a black powder (34 mg, 28%). Mp > 300 °C; ^1H NMR (500 MHz, CS_2, DMSO-d_6) δ 6.94 (m, 4H), 4.86 (s, 4H), 2.39 (t, J = 7.7 Hz, 2H), 1.43 (m, 2H), 1.22−1.05 (br, 10H), 0.7 (t, J = 6.6 Hz, 3H) ppm; ^{13}C NMR (100 MHz, CS_2, DMSO-d_6) δ 153.7, 146.7, 145.7, 145.5, 145.3, 145.0 (2 peaks), 144.7, 144.0, 142.1, 141.7, 141.5, 141.3, 139.7, 135.7, 134.2, 129.0, 116.2, 69.3, 63.0, 35.2, 31.9, 31.6, 29.7, 29.6, 29.4 (2 peaks), 22.9, 14.2; one signal missing/overlapping; MS (MALDI-TOF) *m*/*z* 951 [M^-].

Method 2. Compound **13** (100 mg, 0.31 mmol) and C_{60} (500 mg, 0.69 mmol) were dissolved in 1-chloronaphthalene (10 mL) and sonicated under a stream of argon for 10 min. Then paraformaldehyde (50 mg, 1.67 mmol) and *p*-toluenesulfonic acid (ca. 1 mg) were added, and the mixture was heated to reflux for 2 h. The product was precipitated by the addition of MeOH, filtered, redissolved in 1,2-dichlorobenzene, and subjected to column chromatography (SiO_2, 25% *o*-xylene in cyclohexane) to afford the pure product (74 mg, 25%).

***tert*-Butyl 2-(4-Octylphenylamino)Acetate (15).** 4-Octylaniline **10** (500 mg, 2.43 mmol) and K_2CO_3 (500 mg, 3.6 mmol) were dissolved in DMF (25 mL) and the mixture was stirred for 15 min. Then *tert*-butyl bromoacetate (360 μL, 475 mg, 2.43 mmol) was added all at once and the reaction was stirred overnight at rt. The reaction was stopped by the addition of brine (200 mL) and the product was extracted with heptane (3 × 25 mL), washed with brine, dried (Na_2SO_4), and evaporated to dryness. The crude product was 95% pure as analyzed by GC-MS and could be purified further by column chromatography (SiO_2, 10% EtOAc in heptane). The product **15** was obtained as a colorless oil (450 mg, 60%). IR 3411 (s, N—H stretch), 1733 (s, C═O stretch) cm^{-1}; ^1H NMR (300 MHz, $CDCl_3$) δ 6.99 (d, J = 8.4 Hz, 2H), 6.54 (d, J = 8.4 Hz, 2H), 3.77 (s, 2H), 2.48 (t, J = 7.7 Hz, 2H), 1.6−1.49 (br, 1H), 1.48 (s, 2H), 1.32−1.20 (br, 10H), 0.87 (t, J = 6.7 Hz, 3H) ppm; ^{13}C NMR (75 MHz, $CDCl_3$) δ 170.7, 145.4, 132.7, 129.3, 113.3, 82.0, 47.1, 35.3, 32.1, 32.0, 29.7, 29.5 (two signals), 28.3, 22.9, 14.3 ppm; MS (EI) *m*/*z* 319 [M^+]; HR-MS (ESI) *m*/*z* 320.2580 (M + H^+ calcd for $C_{20}H_{34}NO_2$ 320.2590).

***tert*-Butyl 1-(4-Octylphenyl)fulleropyrrolidine-2-carboxylate (16).** Compound **15** (44 mg, 0.14 mmol), paraformaldehyde (50 mg, 1.7 mmol), and C_{60} (500 mg, 0.69 mmol) were dissolved in 1,2-dichlorobenzene (130 mL) and heated to 130 °C for 2 h. The mixture was then cooled to rt, whereupon Celite was added. The mixture was concentrated in vacuo. The residue was purified by column chromatography (SiO_2, 25% *o*-xylene in cyclohexane) followed by precipitation from *o*-xylene by the addition of MeOH to yield the product **16** as a black powder (12 mg, 8%). ^1H NMR (500 MHz, $CDCl_3$) δ 7.22 (d, J = 8.5 Hz, 2H), 7.11 (d, J = 8.5 Hz, 2H), 6.10 (s, 1H), 5.57 (d, J = 9.4 Hz, 1H), 5.39 (d, J = 9.4 Hz, 1H), 2.62 (t, J = 7.7 Hz, 2H), 1.62 (br m, 2H), 1.42 (s, 9H), 1.40−1.24 (br m, 10H), 0.90 (m, 3H) ppm; ^{13}C NMR (125 MHz, $CDCl_3$) δ 166.8, 151.9, 151.4, 150.2, 147.0, 143.8, 143.7, 142.9, 142.7 (2 peaks), 142.6 (2 peaks), 142.5 (2 peaks), 142.4, 142.3, 142.1, 142.0, 141.9 (3 peaks), 141.7 (2 peaks), 141.6 (5 peaks), 141.0, 140.9 (2 peaks), 140.8, 140.7, 140.5 (2 peaks), 139.4 (2 peaks), 139.0 (3 peaks), 138.9, 138.7, 138.6, 138.5 (2 peaks), 138.4, 138.3 (3 peaks), 138.1 (2 peaks), 137.9, 136.6, 136.5, 136.1, 133.8, 132.4, 132.2, 131.7, 130.8 (2 peaks), 125.8, 111.8, 79.6, 69.4, 68.3, 65.1, 57.8, 45.0, 31.4, 28.2, 25.9, 25.6, 24.5, 19.0 ppm; MS (MALDI-TOF, negative mode) *m*/*z* 1051 [M^-].

4-(Fullero[*c*]pyrrolidin-1-yl)phenyl Trifluoromethanesulfonate (18). To a solution of 4-(fullero[*c*]pyrrolidin-1-yl)phenol (**17**) (115 mg, 0.13 mmol) in dry toluene (10 mL) and dry pyridine (10 mL) at rt was added trifluoromethanesulfonate (73 mg, 0.26 mmol) dropwise. After 5 min, TLC (eluent 25% EtOAc in toluene) showed conversion of all starting material. The mixture was evaporated on Celite and purified by dry column chromatography (SiO_2, (1) heptane−toluene 0−100%; (2) EtOAc−toluene 0−25%) to give the product **18** as a brown solid (116 mg, 90%). Mp > 240 °C; ^{1}H NMR (300 MHz, $CDCl_3$−CS_2 1:1) δ 7.35−7.15 (m, 4H), 5.18 (s, 4H) ppm; ^{13}C NMR (75 MHz, $CDCl_3$−CS_2 1:1) δ 153.8, 147.6, 147.4, 146.4, 146.2, 145.6, 145.4, 144.6, 142.9, 142.7, 142.2, 142.1, 142.0, 140.3, 122.6, 117.1, 69.5, 62.8 ppm; MS (FAB) *m*/*z* 987.84 [M + H$^+$].

***N*-(4-Methoxyphenyl)fullero[*c*]pyrrolidine (19).** To a solution of **17** (31 mg, 0.036 mmol) and K_2CO_3 (15 mg, 17.9 mmol) in dry DMF (5 mL) and dry toluene (5 mL) was added iodomethane (25 mg, 0.18 mmol). The mixture was heated to 40 °C for 12 h and cooled to rt. The solid material was filtered off and the solvent evaporated. The residue was purified by column chromatography (DCVC) with mixtures of toluene/heptane (0−100%) and EtOAc/toluene (0−10%). The product **19** was isolated as a brown powder (9 mg, 30%). Mp > 240 °C; ^{1}H NMR (300 MHz, $CDCl_3$/CS_2 1:1) δ 7.24 (d, J = 8.7 Hz, 2H), 6.99 (d, J = 8.7 Hz, 2H), 5.05 (s, 4H), 3.83 (s, 3H) ppm; ^{13}C NMR (75 MHz, $CDCl_3$−CS_2 1:1) δ 154.4, 146.3, 146.1, 145.9, 145.5, 145.3, 144.5, 142.7, 142.2, 142.1, 141.9, 140.3, 136.3, 118.1, 115.0, 70.0, 64.2, 55.4; MS (MALDI) *m*/*z* 870.04 [M + H$^+$].

2-Nitro-1,4-bis(oct-1-ynyl)benzene (21). 1,4-Dibromo-2-nitrobenzene **20** (10.0 g, 35.6 mmol) was dissolved in a mixture of THF (40 mL), NEt_3 (40 mL), and DMF (4 mL) and the solution was degassed by a flow of N_2(g) while being sonicated in a flask sealed with a septum. [Pd(PPh_3)$_2$$Cl_2$] was then added, followed by another 10 min of degassing, then CuI (30 mg, 0.16 mmol) was added and again the mixture was sonicated for 10 min. Finally 1-octyne (11.6 mL, 8.6 g, 78 mmol) was added, and the solution was heated to 50 °C for 2 h. The reaction was stopped by adding water (250 mL) and the product was extracted with heptane/EtOAc (1:1, 3 × 25 mL), washed with brine, evaporated to dryness, and purified by column chromatography (SiO_2, heptane/EtOAc) to yield the product **21** (9.7 g, 80%) as a yellow oil. ^{1}H NMR ($CDCl_3$, 400 MHz) δ 7.95 (d, J = 1.4 Hz, 1H), 7.48 (dd, J = 8.1 Hz, J = 1.4 Hz, 1H), 7.45 (dd, J = 8.1 Hz, J = 0.4 Hz, 1H), 2.47 (t, J = 7.0 Hz, 2H), 2.41 (t, J = 7.1 Hz, 2H), 1.68−1.53 (br m, 4H), 1.53−1.39 (br m, 4H), 1.39−1.22 (br m, 8H), 0.90 (t, J = 7.0 Hz, 6H) ppm; ^{13}C NMR ($CDCl_3$, 100 MHz) δ 149.7, 134.9, 134.3, 127.1, 124.1, 117.9, 100.5, 94.7, 78.4, 75.8, 31.2 (2 C), 28.5, 28.4, 28.3, 28.2, 22.4 (2 C), 19.8, 19.4, 13.9 (2 C) ppm; MS (EI) *m*/*z* 339 [M$^+$]. Anal. Calcd for $C_{22}H_{29}NO_2$: C 77.84, H 8.61, N 4.13. Found: C 77.86, H 8.99, N 3.83.

2-Amino-1,4-dioctylbenzene (22). Compound **21** (2.23 g; 6.57 mmol) was dissolved in MeOH (50 mL) and EtOAc (50 mL), and then 5% Pd/C (50 mg) was added. The heterogeneous mixture was subjected to H_2 (4 bar) and stirred for 17 h at rt. EtOAc (150 mL) was added, and the mixture was poured through a short column of silica followed by a washing with brine (100 mL). The organic phase was dried with Na_2SO_4 and evaporated to an orange oil of **22** (1.99 g, 95%). ^{1}H NMR (300 MHz, $CDCl_3$) δ 6.95 (d, J = 7.6 Hz, 1H), 6.57 (dd, J = 7.6, 1.7 Hz, 1H), 6.52 (d, J = 1.7 Hz, 1H), 3.56 (br s, 2H), 2.54−2.41 (m, 4H), 1.69−1.49 (m, 4H), 1.47−1.17 (m, 20H), 0.89 (t, J = 6.1 Hz, 6H) ppm; ^{13}C NMR (75 MHz, $CDCl_3$) δ 143.8, 141.7, 129.3, 124.4, 118.9, 115.7, 35.7, 32.0, 31.5, 31.1, 29.8, 29.6, 29.5, 29.4, 29.0, 22.7, 14.2 ppm; GC-MS *m*/*z* 317.4 [M$^+$]; HR-MS (ESI) *m*/*z* 318.3146 (M + H$^+$ calcd for $C_{22}H_{40}N$ 318.3155). Anal. Calcd for $C_{22}H_{39}N$: C 83.21, H 12.38, N 4.41. Found: C 82.92, H 12.69, N 4.36.

2-Chloro-*N*-(2,5-dioctylphenyl)acetamide (23). To a stirred mixture of **22** (1.6 g, 5.0 mmol) and K_2CO_3 (0.83 g, 6.0 mmol) in DMF (40 mL) under argon at 0 °C was added chloroacetyl chloride (0.48 mL, 6.0 mmol). Cooling was stopped, and the reaction was stirred at rt for 3 h before adding brine (100 mL). The resulting reddish precipitate was isolated, washed with water (50 mL), and dried under high vacuum. DCVC (ø 5 cm × 5 cm) with 100% heptane → 100% toluene, 10% increments/40 cm^3 fraction, yielded **23** (1.2 g, 61%) as a white solid. A sample was recrystallized from CH_2Cl_2/heptane resulting in small white needles. Mp 88.5−89.0 °C; R_f 0.14 (40:60, heptane:toluene v/v); IR 3262 (s, NH), 2954 (s, CH), 2922 (s, CH), 2851 (s, CH), 1664 (s, CO) cm^{-1}; ^{1}H NMR (300 MHz, $CDCl_3$) δ 8.28 (br s, 1H), 7.74 (d, J = 1 Hz, 1H), 7.10 (d, J = 8 Hz, 1H), 6.96 (dd, J = 8 Hz, J = 1.5 Hz, 1H), 4.23 (s, 2H), 2.63−2.49 (m, 4H), 1.67−1.51 (m, 4H), 1.44−1.18 (m, 20H), 0.95−0.82 (m, 6H) ppm; ^{13}C NMR (75 MHz, $CDCl_3$) δ 163.8, 141.9, 134.1, 130.8, 129.7, 126.0, 122.7, 43.4, 35.8, 32.0 (×2), 31.6, 31.4, 30.2, 29.7, 29.6, 29.5 (×2), 29.4, 29.3, 22.8 (×2), 14.2 (×2) ppm; HR-MS (ESI) *m*/*z* 416.2701 (M + Na$^+$ calcd for $C_{24}H_{40}ClNONa$ 416.2691). Anal. Calcd for $C_{24}H_{40}ClNO$: C 73.16, H 10.23, N 3.55. Found: C 73.13, H 10.41, N 3.52.

2-Chloro-*N*-(4-nitro-2,5-dioctylphenyl)acetamide (24). To a stirred solution of **23** (4.4 g, 11.2 mmol) and concentrated H_2SO_4 (15.4 mL, 28.9 mmol) in glacial acetic acid (200 mL) under argon at 0 °C was added fuming nitric acid (0.51 mL, 12.3 mmol). Cooling was stopped and the reaction was stirred at 55 °C for 1 h before the reaction was stopped by adding ice (100 g). The resulting mixture was extracted with 50:50 (v/v) heptane:EtOAc (3 × 75 mL), and the combined organic phase was dried with Na_2SO_4 and evaporated in vacuo. DCVC (ø 5 cm × 5 cm) with 100% heptane → 100% toluene, 10% increments/40 cm^3 fraction, yielded **24** (2.2 g, 45%) as a light yellow solid. A sample was recrystallized from methanol/water resulting in small white needles. Mp 99.5−100.0 °C; R_f 0.11 (50:50, heptane:toluene v/v); IR 3256 (s, NH), 2924 (s, CH), 2851 (s, CH), 1668 (s, CO), 1519 (s, NO_2), 1352 (s, NO_2) cm^{-1}; ^{1}H NMR (300 MHz, $CDCl_3$) δ 8.51 (br s, 1H), 8.18 (s, 1H), 7.80 (s, 1H), 4.26 (s, 2H), 2.92−2.83 (m, 2H), 2.66−2.57 (m, 2H), 1.70−1.55 (m, 4H), 1.46−1.17 (m, 20H), 0.93−0.81 (m, 6H) ppm; ^{13}C NMR (75 MHz, $CDCl_3$) δ 163.9, 145.2, 138.5, 137.9, 130.6, 126.2 (*C*H), 123.6 (*C*H), 43.4 (*C*H_2Cl), 33.4, 32.0, 31.9, 31.0, 30.8, 29.8, 29.5, 29.4 (×3), 29.3 (×2), 22.8, 22.7, 14.2 (×2) ppm; HR-MS (ESI) *m*/*z* 461.2552 (M + Na$^+$ calcd for $C_{24}H_{39}ClN_2O_3Na$ 461.2541). Anal. Calcd for $C_{24}H_{39}ClN_2O_3$: C 65.66, H 8.95, N 6.38. Found: C 65.33, H 9.12, N 6.29.

***N*-(4-Amino-2,5-dioctylphenyl)-2-chloroacetamide (25).** To an argon-deoxygenized stirred mixture of **24** (0.44 g, 1.0 mmol) in CH_2Cl_2 (100 mL) and water (100 mL) were added K_2CO_3 (0.69 g, 5.0 mmol) and $Na_2S_2O_4$ (0.87 g, 5.0 mmol). The mixture was again deoxygenated, 1,1′-diethyl-4,4′-bipyridinium dibromide (0.11 g, 0.30 mmol) was added, and the flask was fitted with a suitable stopper and heated to 50 °C for 40 h. After allowing the mixture to cool to rt, the phases were separated and the aqueous phase was extracted with CH_2Cl_2 (60 mL). The combined organic phase was extracted with brine (3 × 40 mL), dried with Na_2SO_4, and evaporated in vacuo, resulting in **25** (0.32 g, 78%) as a brown viscous oil (pure on ^{1}H NMR). The oil can be used directly in the next step or purified by DCVC (ø 5 cm ×5 cm) with 100% heptane → 100% EtOAc, 10% increments/40 cm^3 fraction, to yield **25** (0.16 g, 39%) as a white solid. The product should not be subjected to high vacuum as it will degrade over time. A sample was recrystallized from ethanol/water resulting in white crystals. Mp 98.5−99.0 °C; R_f 0.63 (50:50, heptane:EtOAc v/v); IR 3425 (m, NH amine), 3328 (m, NH amine), 3255 (s, NH amide), 2950 (s, CH), 2922 (s, CH), 2852 (s, CH), 1657 (s, NH amide), 1538 (s, NH amine) cm^{-1}; ^{1}H NMR (300 MHz, $CDCl_3$) δ 8.04 (br s, 1H), 7.33 (s, 1H), 6.51 (s, 1H), 4.19 (s, 2H), 3.69 (s, 2H), 2.51−2.38 (m, 4H), 1.66−1.47 (m, 4H), 1.42−1.18 (m, 20H), 0.94−0.83 (m, 6H) ppm; ^{13}C NMR

(75 MHz, $CDCl_3$) δ 164.2, 142.5, 134.3, 125.5, 125.5, 125.1, 116.4, 43.1, 32.0, 31.9, 31.3, 31.0, 30.3, 29.8, 29.6, 29.6, 29.5, 29.3, 29.3, 28.8, 22.7 (×2), 14.2 (×2) ppm; HR-MS (ESI) m/z 431.2827 ($M + Na^+$ calcd for $C_{24}H_{41}ClN_2ONa$ 431.2800). Anal. Calcd for $C_{24}H_{41}ClN_2O$: C 70.47, H 10.10, N 6.85. Found: C 70.54, H 10.30, N 6.78.

***N*,*N*′-(2,5-Dioctyl-1,4-phenylene)bis(2-chloroacetamide) (26).** To a stirred solution of **25** (0.13 g, 0.32 mmol) in CH_2Cl_2 (10 mL) under argon was added chloroacetic anhydride (0.50 g, 3.0 mmol). After 10 min of stirring, a precipitate formed, and after 3 h the mixture was evaporated in vacuo. The solid was dissolved in THF and evaporated on Celite. DCVC (ø 5 cm × 5 cm) with 100% heptane → 100% THF, 10% increments/40 cm^3 fraction, followed by THF elution until no **26** remained on the column, yielded **26** (0.11 g, 71%) as a white solid. The product should not be subjected to high vacuum as it will degrade over time. A sample was recrystallized from THF/water resulting in white crystals. Mp 216.0−217.0 °C; R_f 0.55 (50:50, heptane:EtOAc v/v); IR 3262 (s, NH amide), 2952 (s, CH), 2924 (s, CH), 2853 (s, CH), 1662 (s, NH amide) cm^{-1}; ^1H NMR (300 MHz, $CDCl_3$) δ 8.27 (br s, 2H), 7.83 (s, 2H), 4.23 (s, 4H), 2.61−2.54 (m, 4H), 1.65−1.49 (m, 4H), 1.44−1.17 (m, 20H), 0.91−0.81 (m, 6H) ppm; ^{13}C NMR (75 MHz, $CDCl_3$) δ 163.7 (×2), 132.2 (×2), 131.8 (×2), 123.8 (×2), 43.4 (×2), 32.1 (×2), 31.6 (×2), 30.2 (×2), 29.8 (×2), 29.6 (×2), 29.4 (×2), 22.9 (×2), 14.3 (×2) ppm; HR-MS (ESI) m/z 507.2541 ($M + Na^+$ calcd for $C_{26}H_{42}Cl_2N_2O_2Na$ 507.2516). Anal. Calcd for $C_{26}H_{42}Cl_2N_2O_2$: C 64.32, H 8.72, N 5.77. Found: C 64.04, H 8.85, N 5.66.

***N*^{1},*N*^{4}-Bis(2-chloroethyl)-2,5-dioctylbenzene-1,4-diamine (27).** To a stirred mixture of **26** (0.23 g, 0.47 mmol) in THF (50 mL) under argon at 0 °C was added borane−dimethyl sulfide complex (0.40 mL, 4.0 mmol). Cooling was stopped and after 16 h, methanol (10 mL) was added to the clear solution. When hydrogen formation ceased, heptane (25 mL) and water (25 mL) were added, the phases were separated, and the aqueous phase was extracted with heptane (2 × 25 mL). The combined organic phase was dried with Na_2SO_4 and evaporated in vacuo, yielding **27** (0.18 g, 83%) as a colorless oil. Compound **27** is unstable and should not be stored, and subjecting it to high vacuum causes polymerization. R_f 0.63 (heptane/EtOAc 7:3); ^1H NMR (300 MHz, $CDCl_3$) δ 6.46 (s, 2H), 3.74 (t, J = 5.5 Hz, 4H), 3.48 (t, J = 5.5 Hz, 4H), 2.51−2.29 (m, 4H), 1.65−1.48 (m, 4H), 1.44−1.17 (m, 20H), 0.93−0.81 (m, 6H) ppm; ^{13}C NMR (75 MHz, $CDCl_3$) δ 136.9 (×2), 127.6 (×2), 114.8 (×2), 47.2 (×2), 44.0 (×2), 32.0 (×2), 31.4 (×2), 29.9 (×2), 29.8 (×2), 29.6 (×2), 29.4 (×2), 22.8 (×2), 14.2 (×2) ppm; HR-MS (ESI) m/z 457.3116 ($M + H^+$ calcd for $C_{26}H_{47}Cl_2N_2$ 457.3111).

1,1′-(2,5-Dioctyl-1,4-phenylene)bis(aziridine) (28). To a stirred mixture of NaH (0.006 g, 60 wt % dispersion in mineral oil, 0.15 mmol) in DMSO (10 mL) under argon was added **27** dissolved in DMSO (5 mL). The mixture was heated to 50 °C, and after 3 h, heating was stopped and the reaction was allowed to reach rt before it was extracted with heptane (3 × 20 mL). The combined organic phase was washed with water (20 mL), dried with Na_2SO_4, and evaporated in vacuo, yielding **28** (0.23 g; quantitative, corrected) as light yellow crystals containing mineral oil as the only impurity. The crude product can be used for the next step without further purification. A sample was dissolved in CH_2Cl_2, evaporated on Celite, and put on a pad of silica gel 60 (0.015−0.040 mm). Elution with heptane followed by heptane/THF 70:30 (v/v) afforded pure **28**. The product should not be subjected to high vacuum as it will polymerize. Recrystallization from methanol/water resulted in small white needles. Mp 67.5−68.0 °C; R_f 0.49 (80:20, heptane:THF v/v); IR 2982 (s, aziridine), 2954 (s, CH), 2923 (s, CH), 2853 (s, CH), 1285 (s, aziridine), 1166 (m, aziridine) cm^{-1}; ^1H NMR (300 MHz, $CDCl_3$) δ 6.60 (s, 2 H), 2.70−2.62 (m, 4H), 2.05 (br s, 8 H), 1.71−1.58 (m, 4 H), 1.46−1.22 (m, 20 H), 0.93−0.84 (m, 6 H) ppm; ^{13}C NMR (75 MHz, $CDCl_3$) δ 146.6 (×2), 133.1 (×2), 120.7 (2 × *C*H), 32.1 (×2), 30.9 (× 2), 30.2 (×2), 29.8 (×2), 29.7 (×2), 29.5 (×2), 28.2 (×4), 22.8 (×2), 14.3 (×2) ppm; HR-MS (ESI) m/z 385.3583 ($M + H^+$ calcd for $C_{26}H_{45}N_2$ 385.3577). Anal. Calcd for $C_{26}H_{44}N_2$: C 81.19, H 11.53, N 7.28. Found: C 80.85, H 11.98, N 7.18.

4-Iodo-2,5-dioctylaniline (30). To a solution of 2,5-dioctylaniline **22** (1.87 g, 5.9 mmol) in CH_2Cl_2 (4 mL) and methanol (4 mL) was added $NaHCO_3$ (0.99 g, 11.8 mmol), and the mixture was cooled to 0 °C under an argon atmosphere. A solution of benzyltrimethylammonium dichloroiodate (2.05 g, 5.9 mmol) in CH_2Cl_2 was added dropwise over 15 min. The mixture was allowed to warm to rt and stirred for an additional 20 min and then quenched by addition of water (15 mL). The organic phase was separated and washed with water (3 × 5 mL), dried over $MgSO_4$, and evaporated. The residue was purified by dry column vacuum chromatography (DCVC) with EtOAc (0−10%) and heptane, affording the product **30** as a light brown oil, which solidified when kept at +4 °C (2.09 g, 80%). Mp 30−31 °C; ^1H NMR ($CDCl_3$, 300 MHz) δ 7.40 (s, 1H), 6.55 (s, 1H), 3.57 (br s, 2H), 2.55 (t, J = 8.1 Hz, 2H), 2.38 (t, J = 7.8 Hz, 2H), 1.62−1.48 (m, 4H), 1.41−1.20 (m, 20H), 0.88 (t, J = 6.3 Hz, 6H) ppm; ^{13}C NMR ($CDCl_3$, 100 MHz) δ 144.5, 143.6, 139.5, 127.3, 116.5, 86.7, 40.5, 32.1, 32.0, 30.7, 30.6, 29.7, 29.6, 29.6, 29.4, 29.4, 28.8, 22.8, 22.8, 14.3, 14.3 ppm; MS (EI) m/z 443 [M^+]. Anal. Calcd for $C_{22}H_{38}IN$: C 59.59; H 8.64; N 3.16. Found: C 59.63; H 8.78; N 3.08.

4-Triisopropylsilylethynyl-2,5-dioctylaniline (31). A solution of 4-iodo-2,5-dioctylaniline (**30**) (76 mg, 0.17 mmol), [Pd-$(PPh_3)_2Cl_2$] (6 mg, 0.01 mmol), CuI (0.3 mg, 0.017 mmol), and triisopropylsilylacetylene (0.4 mL, 1.7 mmol) in dry, degassed diisopropylamine (1 mL) and dry, degassed THF (3 mL) was placed under an argon atmosphere and heated to 100 °C for 5 min by microwave irradiation. The resulting dark solution was cooled to rt, the solvents were evaporated, and the residue was purified by dry column vacuum chromatography (DCVC) with EtOAc (0−5%) and heptane, affording the product **31** as a light brown oil (76 mg, 90%). ^1H NMR ($CDCl_3$, 300 MHz) δ 7.14 (s, 1H), 6.47 (s, 1H), 3.69 (br s, 2H), 2.69 (t, J = 7.5 Hz, 2H), 4.41 (t, J = 7.5 Hz, 2H), 1.66−1.54 (m, 4H), 1.40−1.24 (m, 23H), 1.14 (s, 18H), 0.89 (t, J = 6.6 Hz, 6H) ppm; ^{13}C NMR ($CDCl_3$, 100 MHz) δ 144.7, 144.6, 134.1, 124.3, 115.6, 112.8, 107.0, 90.6, 34.9, 32.1, 32.0, 31.2, 30.9, 29.9, 29.9, 29.8, 29.7, 29.5, 29.4, 29.2, 29.0 ppm. Anal. Calcd for $C_{33}H_{59}NSi$: C 79.60, H 11.94, N 2.81. Found: C 79.51, H 11.59, N 2.56%.

***tert*-Butyl 2-(4-iodo-2,5-dioctylphenylamino)acetate (32).** To a solution of 4-iodo-2,5-dioctylaniline **30** (83 mg, 0.187 mmol) and *tert*-butyl bromoacetate (365 mg, 1.8 mmol) in dry DMF (3 mL) was added K_2CO_3 (250 mg, 1.8 mmol). The mixture was heated to 60 °C for 6 h and cooled to rt. Water (10 mL) was added and the mixture was extracted with EtOAc−heptane (1:3, 3 × 5 mL). The combined organic phases were dried over $MgSO_4$ and evaporated. The residue was purified by dry column vacuum chromatography (DCVC) with toluene (0−10%) and heptane. The product **32** was obtained as a light red-brown oil (78 mg, 75%). ^1H NMR ($CDCl_3$, 300 MHz) δ 7.40 (s, 1H), 6.32 (s, 1H), 4.26 (br s, 1H), 3.80 (s, 2H), 2.59 (t, J = 7.8 Hz, 2H), 4.43 (t, J = 7.5 Hz, 2H), 1.64−1.51 (m, 4H), 1.50 (s, 9H), 1.42−1.21 (m, 20H), 0.89 (t, J = 6.3 Hz, 6H) ppm; ^{13}C NMR ($CDCl_3$, 100 MHz) δ 170.1, 145.0, 143.6, 139.0, 127.2, 111.5, 85.5, 82.1, 46.5, 40.9, 32.0, 32.0, 30.6, 30.4, 29.7, 29.6, 29.5, 29.4, 29.3, 28.6, 28.2, 22.8, 22.8, 14.2 ppm; MS (EI) m/z 557 [M^+]; HR-MS (ESI) m/z 558.2808 ([$M + H$]$^+$ calcd for $C_{28}H_{49}INO_2$ 558.2808).

9,9-Didecyl-9*H*-fluorene (34). NaH (10.0 g, 60 wt %, 0.25 mol) was added to DMF (250 mL) and the mixture was heated to 50 °C for 1 h and then cooled to rt again. Fluorene **33** (10 g, 60 mmol) and decyl bromide (27 mL, 29 g, 132 mmol) were added all at once, and the solution was left overnight at rt. Then

the reaction was quenched with brine, the product extracted (3 × 100 mL heptane), and the combined organic phases dried ($MgSO_4$) and evaporated to a colorless oil, which was purified by dry column chromatography (gradient from heptane to 10% EtOAc in heptane) to afford the product **34** (19.9 g, 75%). ^{1}H NMR (400 MHz, $CDCl_3$) δ 7.69 (d, J = 7.34 Hz, 2H), 7.36−7.21 (m, 6 H), 2.00−1.88 (m, 4 H), 1.34−0.95 (m, 32 H), 0.90−0.80 (m, 6 H) ppm; ^{13}C NMR (100 MHz, $CDCl_3$) δ 150.9, 141.3, 127.2, 126.9, 123.0, 119.8, 55.2, 40.6, 32.1, 30.3, 29.8 (2 peaks), 29.5 (2 peaks), 24.0, 22.9, 14.3 ppm; MS (GC-MS) m/z 446.5 [M^+], 305.3 ([$M - C_{10}H_{21}$]$^+$).

9,9-Didecyl-2,7-dinitro-9*H*-fluorene (35). 9,9-Didecylfluorene **34** (1.0 g, 2.24 mmol) was added dropwise to an ice-cooled mixture of glacial acetic acid (5 mL) and fuming nitric acid (5 mL) while the temperature was kept below 10 °C. The solution was stirred at rt until the next day and was then quenched with ice water, extracted (3 × 25 mL EtOAc/heptane, 50:50), dried ($MgSO_4$), evaporated to dryness, purified by column chromatography (SiO_2, 5% EtOAc in heptane), and recrystallized from MeOH to yield **35** as yellow crystals (550 mg, 46%). Mp 64−65 °C; IR 3090 (w, aryl C−H stretch), 2925, 2853 (s, alkane C−H stretch), 1520, 1339 (s, nitro N−O stretch) cm^{-1}; ^{1}H NMR (300 MHz, $CDCl_3$) δ 8.33 (dd, J = 8.4 Hz, J = 2.1 Hz, 2H), 8.27 (d, J = 2.1 Hz, 2H), 7.92 (d, J = 8.4 Hz, 2H), 2.10 (m, 4H), 1.31−0.95 (br, 32H), 0.84 (t, J = 6.9 Hz) ppm; ^{13}C NMR (75 MHz, $CDCl_3$) δ 153.7, 148.6, 144.9, 123.8, 121.8, 118.7, 56.7, 40.0, 32.1, 29.9, 29.7 (2 peaks), 29.4 (2 peaks), 24.0, 22.9, 14.3 ppm; MS (ES) m/z 559.4 ([$M + Na^+$]). Anal. Calcd for $C_{33}H_{48}N_2O_4$: C 73.84, H 9.01, N 5.22. Found: C 73.55, H 9.02, N 5.26.

9,9-Didecyl-9*H*-fluorene-2,7-diamine (36). Compound **35** (1.0 g, 1.86 mmol) was dissolved in EtOAc (20 mL) and Pd/C (20 mg, 10% Pd on carbon) was added, then the mixture was shaken in a Parr hydrogenator at 4 bar of hydrogen overnight. The solution was filtered and evaporated to an oil, which was purified by column chromatography (10% EtOAc in toluene) to yield the product **36** as a red oil (700 mg, 90%). IR 3459 (N−H stretch), 3370 (N−H stretch), 3030 (w), 3004 (w), 2925 (s), 2852 (s), 1618 (s), 1468 (s), 808 (m) cm^{-1}; ^{1}H NMR (400 MHz, $CDCl_3$) δ 7.33 (d, J = 7.8 Hz, 2H), 6.66−6.59 (m, 4H), 1.85−1.78 (m, 4H), 1.30−0.98 (m, 32H), 0.85 (t, J = 7.0 Hz, 6H) ppm; ^{13}C NMR (100 MHz, $CDCl_3$) δ 151.8, 144.5, 133.4, 119.2, 114.1, 110.3, 54.8, 41.1, 32.1, 30.5, 29.9, 29.8, 29.6, 29.5, 24.0, 22.9, 14.3 ppm; MS (EI) m/z 476.5 [M^+]; HR-MS m/z 477.4226 ($M + H^+$ calcd for $C_{33}H_{53}N_2$ 477.4209).

***N*,*N*′-(9,9-Didecyl-9*H*-fluorene-2,7-diyl)bis(2-chloroacetamide) (37).** The diamine **36** (500 mg, 1.05 mmol) and K_2CO_3 (320 mg, 2.3 mmol) were dissolved in DMF (20 mL) and the mixture was cooled on an ice bath. Chloroacetyl chloride (250 mg, 176 μL, 2.2 mmol) was added dropwise during 30 min, and the reaction was then left at rt overnight. The reaction was quenched with brine (200 mL) and the product was extracted (Et_2O, 3 × 20 mL), dried (Na_2SO_4), evaporated to dryness, and purified by column chromatography (SiO_2, 20% EtOAc in heptane) to yield the diamide **37** as a yellow wax (632 mg, 96%). IR 3399 (w), 3299 (m, N−H stretch), 2926 (s), 2853 (s), 1667 (s, C=O stretch), 1698 (m), 1616 (m), 1549 (s), 1469 (s), 819 (m, C−Cl stretch) cm^{-1}; ^{1}H NMR (300 MHz, $CDCl_3$) δ 8.23 (s, 2H), 7.62 (d, J = 8.2 Hz, 2H), 7.56 (d, J = 1.8 Hz, 2H), 7.50 (dd, J = 8.2 Hz, J = 1.8 Hz, 2H), 4.22 (s, 4H), 1.95 (m, 4H), 1.32−0.95 (m, 32H), 0.85 (t, J = 6.9 Hz, 6H) ppm; ^{13}C NMR (100 MHz, $CDCl_3$) δ 163.7, 152.2, 137.9, 136.0, 120.1, 119.0, 114.8, 55.8, 43.2, 40.6, 32.1, 30.3, 29.8, 29.7, 29.6, 29.5, 24.0, 22.9, 14.3 ppm; MS (FAB) m/z 628 [M^+]. Anal. Calcd for $C_{37}H_{54}Cl_2N_2O_2$: C 70.57, H 8.64, N 4.45. Found: C 70.42, H 8.68, N 4.31.

***N*^{2},*N*^{7}-Bis(2-chloroethyl)-9,9-didecyl-9*H*-fluorene-2,7-diamine (38).** The chloroethyl amide **37** (600 mg, 0.95 mmol) was dissolved in dry and degassed THF (40 mL) and the mixture was cooled to 0 °C under an atmosphere of argon. Borane−dimethyl sulfide complex (1 mL; 10 mmol) was then added dropwise and the reaction was left at rt overnight. Excess borane was destroyed by careful addition of MeOH (5 mL) and the solution was stirred until no more hydrogen gas evolved (1 h). The product was purified by aqueous workup and extraction (heptane), followed by column chromatography (SiO_2, toluene) to yield the product **38** as a red oil (489 mg, 85%) that quickly turned black upon standing. ^{1}H NMR (300 MHz, $CDCl_3$) δ 7.37 (d, J = 8.6 Hz, 2H), 6.61−6.54 (m, 4H), 4.17−3.91 (br, 2H), 3.75 (t, J = 5.8 Hz, 4H), 3.55 (t, J = 5.8 Hz, 4H), 1.83 (m, 4H), 1.33−0.99 (m, 32H), 0.85 (t, J = 6.9 Hz, 6H) ppm; ^{13}C NMR (75 MHz, $CDCl_3$) δ 151.9, 145.8, 133.1, 119.4, 112.2, 108.6, 55.0, 46.3, 43.9, 41.1, 32.1, 30.4, 29.9, 29.8, 29.6, 29.5, 24.0, 22.9, 14.3 ppm; MS (FAB) m/z 600 [M^+].

1,1′-(9,9-Didecyl-9*H*-fluorene-2,7-diyl)diaziridine (39). Sodium hydride (30 mg, 60 wt % in oil, 1.5 mmol) was added to DMSO (12 mL), and the mixture was stirred for 1 h under an atmosphere of argon. Then chloroethyl amine **38** (300 mg, 0.5 mmol) was dissolved in DMSO (6 mL) and added dropwise to the sodium hydride mixture. After 15 min, the solution was heated to 40 °C and stirred overnight and then quenched with brine (200 mL). The product was extracted (3 × 25 mL, 50% EtOAc in heptane), dried (Na_2SO_4), evaporated to dryness, and purified by column chromatography (SiO_2, 10% NEt_3 in heptane) to yield **39** as a stable, light yellow oil (197 mg, 75%). ^{1}H NMR (400 MHz, $CDCl_3$) δ 7.43 (d, J = 8.0 Hz, 2H), 6.94 (br, 2H), 6.93 (dd, J = 8.0 Hz, J = 2.0 Hz, 2H), 2.13 (s, 4 H) 1.87 (m, 4H), 1.30−1.00 (br, 32H), 0.85 (t, J = 7.1 Hz, 6H) ppm; ^{13}C NMR (100 MHz, $CDCl_3$) δ 154.1, 151.8, 136.0, 119.7, 119.3, 115.8, 55.0, 40.7, 32.1, 30.3, 29.8 (2 peaks), 29.5 (2 peaks), 28.2, 23.9, 22.9, 14.3 ppm; MS (FAB) m/z 528 [M^+]; HR-MS m/z 529.4509 ($M + H^+$ calcd for $C_{37}H_{57}N_2$ 529.4522).

2,7-Bis(fullero[*c*]pyrrolidin-1-yl]-9,9′-didecyl-9*H*-fluorene (40). Method I. C_{60} (200 mg, 0.28 mmol) and the diaziridine **39** (20 mg, 0.04 mmol) were dissolved in 1,2-dichlorobenzene (10 mL) and the solution was sonicated under a stream of argon for 10 min. The solution was heated to 200 °C in a sealed glass tube for 15 h and then cooled to rt. The product, along with unreacted C_{60}, was precipitated by the addition of MeOH and then purified by column chromatography (SiO_2, cyclohexane/*o*-xylene) to yield the product **40** as a black powder (4 mg, 5%). IR 2921 (s), 2849 (m), 1611 (m), 1465 (m), 526 (m) cm^{-1}; ^{1}H NMR (500 MHz, $CDCl_3$) δ 7.42 (d, J = 8.0 Hz, 2 H), 7.00 (m, 2H), 6.97 (m, 2H), 5.00 (s, 8H), 1.90−1.83 (m, 4H), 1.06−0.88 (m, 32H), 0.66−0.57 (m, 6H) ppm; ^{13}C NMR (125 MHz, $CDCl_3$) δ 154.3, 147.4, 146.4, 146.2, 145.9, 145.7, 145.4, 144.6, 143.2, 142.8, 142.3, 142.2, 142.0, 140.4, 136.3 (one fullerene signal missing), 69.9, 63.7, 32.5, 30.4, 30.3 (2 signals), 30.23 (2 signals), 30.0 (2 signals), 23.5, 14.8 ppm; MS (MALDI-TOF, negative mode) m/z 1970 [M^-].

Method II. C_{60} (500 mg; 0.69 mmol), paraformaldehyde (25 mg, 0.8 mmol), and compound **42** (60 mg, 0.07 mmol) were dissolved in 1-chloronaphthalene (10 mL), and the mixture was sonicated under a stream of argon for 10 min. The mixture was refluxed under an atmosphere of nitrogen for 120 min and was then cooled to rt. The product, along with unreacted C_{60}, was precipitated by the addition of MeOH, and the product was purified by column chromatography (SiO_2, cyclohexane, *o*-xylene) to yield **40** as a black powder (13 mg, 14%).

***tert*-Butyl 9,9-didecyl-9*H*-fluorene-2,7-diyldicarbamate (41).** Compound **36** (238 mg; 0.5 mmol), $(Boc)_2O$ (218 mg; 1 mmol), and $NaHCO_3$ (250 mg; 3 mmol) were added to isopropyl alcohol (5 mL), and the mixture was sonicated at rt for 2 h. The solution was diluted with water (50 mL) and the product was extracted with heptane (3 × 10 mL) and then purified by column chromatography (SiO_2, EtOAc, heptane) to yield **41** as a white solid (310 mg, 92%). ^{1}H NMR ($CDCl_3$, 300 MHz) δ 7.52 (d, J = 8 Hz, 2H), 7.31 (br, 4H), 6.54 (2H), 1.89 (m, 2H), 1.54 (s, 18H),

1.28−0.98 (br, 32H), 0.85 (t, J = 6.8 Hz, 6H) ppm; ^{13}C NMR ($CDCl_3$, 75 MHz) δ 152.9, 151.8, 137.2, 136.3, 119.6, 117.3, 113.3, 80.5, 55.5, 40.7, 32.1, 30.3, 29.8 (2 peaks), 29.5 (2 peaks), 28.6, 23.9, 22.9, 14.3 ppm; HR-MS (ESI) m/z 699.5059 (M + Na^+ calcd for $C_{43}H_{68}N_2O_4Na$ 699.5077). Anal. Calcd for $C_{43}H_{68}N_2O_4$: C 76.29, H 10.12, N 4.14. Found: C 76.33, H 10.37, N 4.07.

***tert*-Butyl 2,2′-(9,9-didecyl-9*H*-fluorene-2,7-diyl)bis(*tert*-butoxycarbonylazanediyl)diacetate (42).** Compound **41** (200 mg; 0.295 mmol) was dissolved in DMF (5 mL) and cooled to 0 °C. Then NaH (12 mg, 60 wt % in oil, 0.3 mmol) was added and the solution was stirred under argon, while *tert*-butyl bromoacetate (45 μL, 59 mg, 0.30 mmol) was added dropwise. After 20 min, another portion of NaH (12 mg) was added, followed by *tert*-butyl bromoacetate (45 μL). The solution was allowed to reach rt and was then diluted with water (50 mL) and the product was extracted with EtOAc (3 × 10 mL). The crude product was purified by column chromatography (SiO_2, NEt_3/heptane) to give **42** as a colorless oil (220 mg, 82%). ^{1}H NMR (300 MHz, $CDCl_3$) δ 7.58 (d, J = 8.2 Hz, 2H), 7.27−7.22 (m, 4H), 4.21 (s, 4H), 2.04−1.78 (m, 4H), 1.48 (s, 18H), 1.42 (s, 18H), 1.28−0.93 (m, 32H), 0.84 (t, J = 6.6 Hz, 6H) ppm; ^{13}C NMR (75 MHz, $CDCl_3$) δ 169.2, 154.8, 151.6, 142.2, 138.8, 125.2, 119.8, 81.7, 80.7, 55.4, 53.4, 40.7, 32.1, 30.4, 29.9, 29.6, 29.4, 28.5, 28.3, 24.1, 22.8, 14.3 ppm; HR-MS (ESI) m/z 927.6453 (M + Na^+ calcd for $C_{55}H_{88}N_2O_8Na$ 927.6438).

Acknowledgment. The research leading to these results has received funding from the European Community's Seventh Framework Programme (FP7/2007-2013) under the grant agreement "SINGLE" no. 213609, the Danish-Chinese Center for Molecular Nano-Electronics funded by the Danish Basic Research Foundation, and The Danish Research Council for Independent Research|Natural Sciences (no. 09-062281). The work in Mons is also supported by the Interuniversity Attraction Pole IAP 6/27 Program of the Belgian Federal Government. J.C. is funded by the Belgian National Fund for Scientific Research (FNRS).

Supporting Information Available: NMR and spectroscopic data, complete ref 36, computational data (coordinates), HPLC analytical data for compounds **1**, **14**, **16**, **18**, **19**, and **40**, and synthetic protocols for compounds **9** and **10**. This material is available free of charge via the Internet at http://pubs.acs.org.